125 Jahre Röntgen – Wo stehen wir heute?

Aktuelle Entwicklungen auf dem Gebiet der CT

Marc Kachelrieß

Abteilung für Röntgenbildgebung und CT
Deutsches Krebsforschungszentrum (DKFZ)
www.dkfz.de/ct

DEUTSCHES KREBSFORSCHUNGSZENTRUM
IN DER HELMHOLTZ-GEMEINSCHAFT

Content

- Prefilters for dose reduction
- Photon counting
- Deep learning (in image formation)
- Motion compensation

Prefilters for Dose Reduction

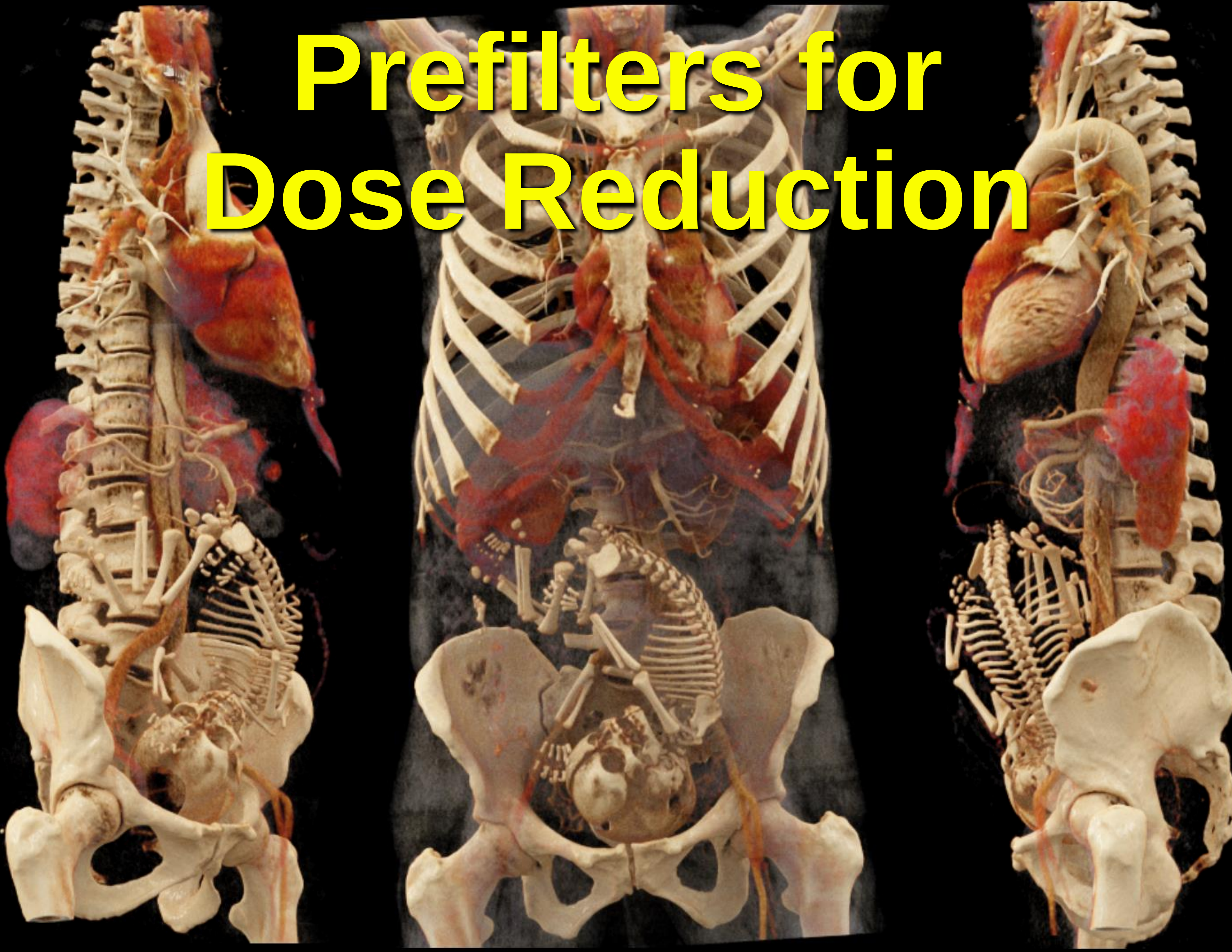

Aortic dissection during pregnancy. Image courtesy of PD Dr. Matthias May, University of Erlangen-Nürnberg, Germany.

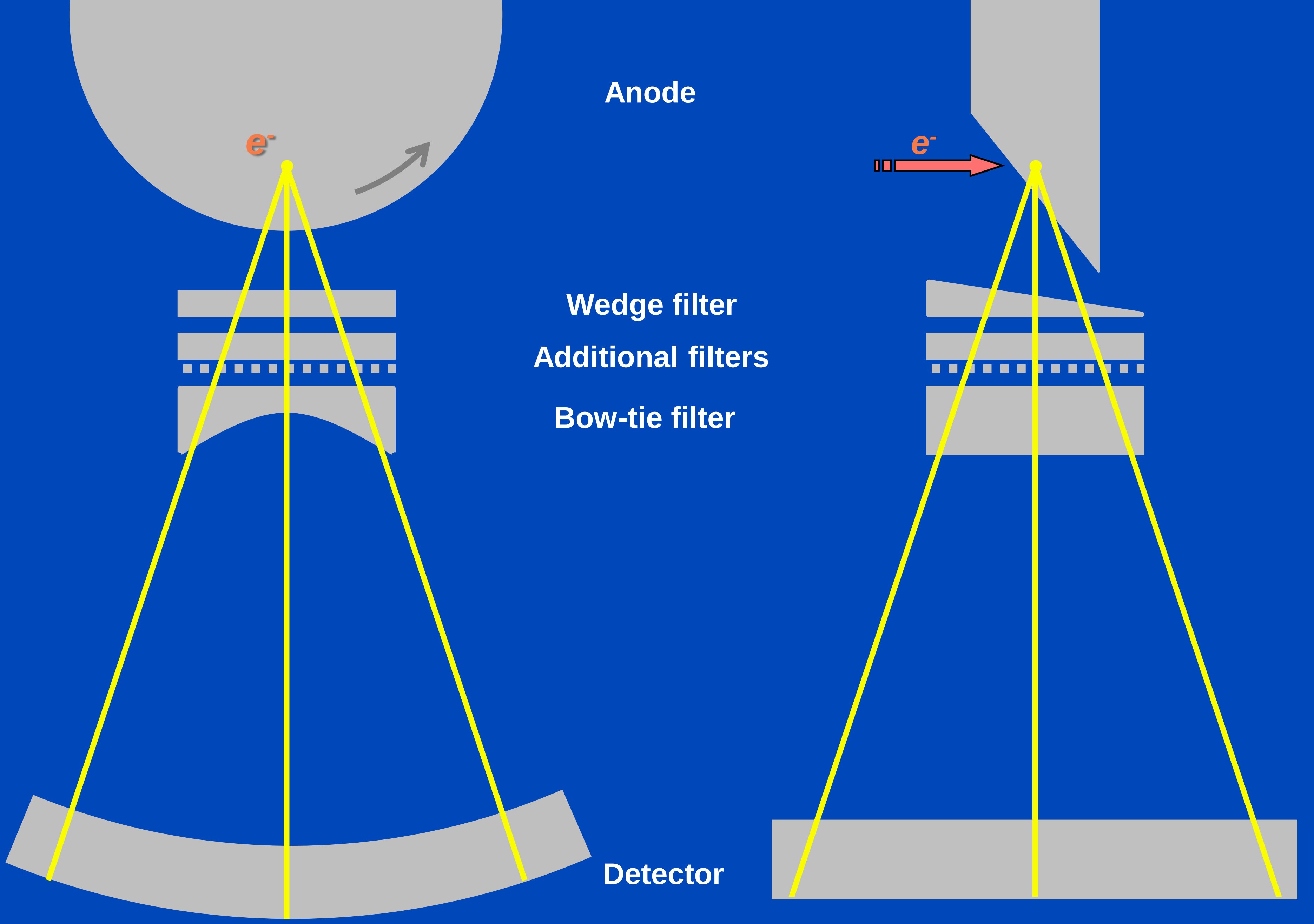

Figure not drawn to scale. Type and order of prefiltration may differ from scanner to scanner.
Depending on the selected protocol filters are changed automatically (e.g. small bowtie for pediatric scans).

120 kV + 0 mm water with and without prefilter

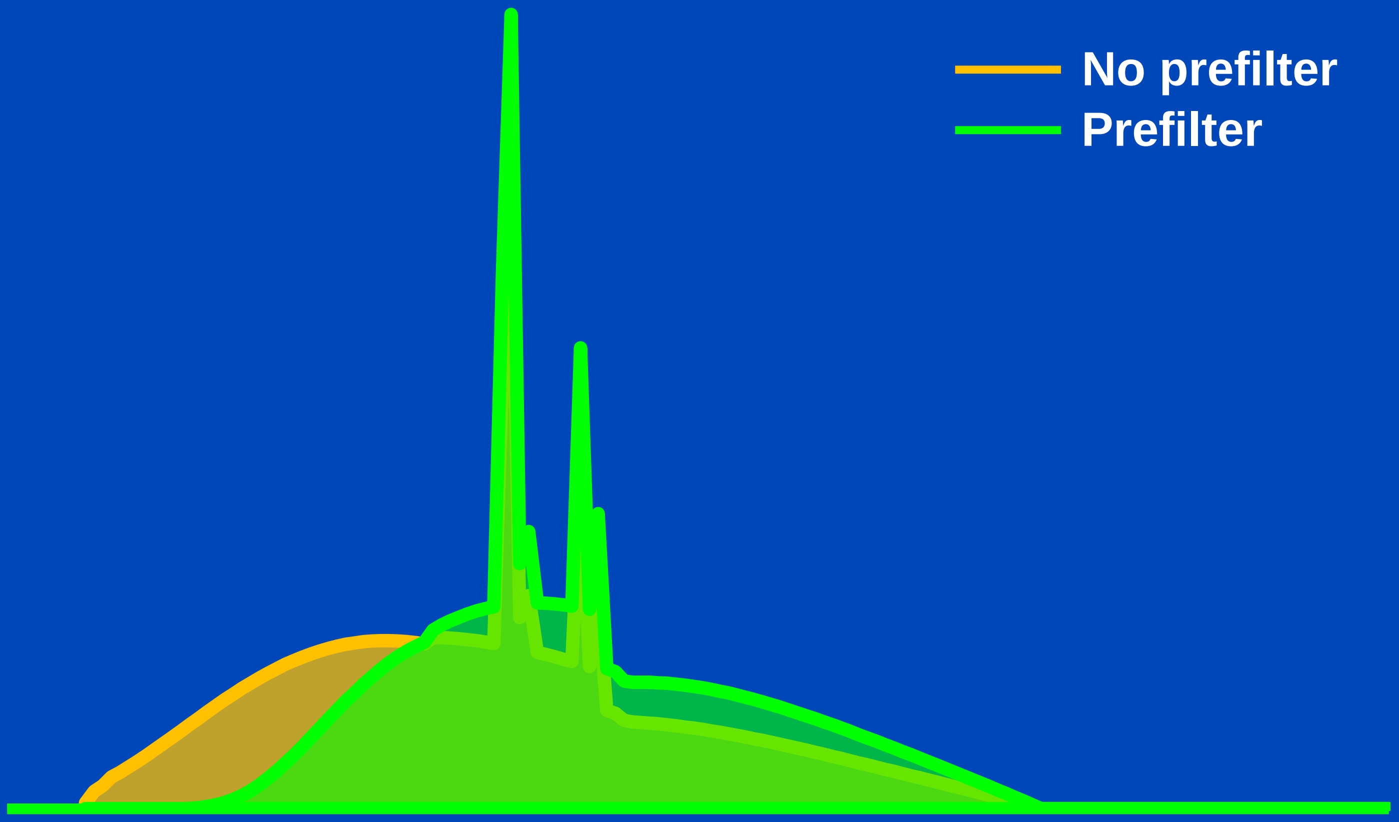

120 kV + 320 mm water with and without prefilter

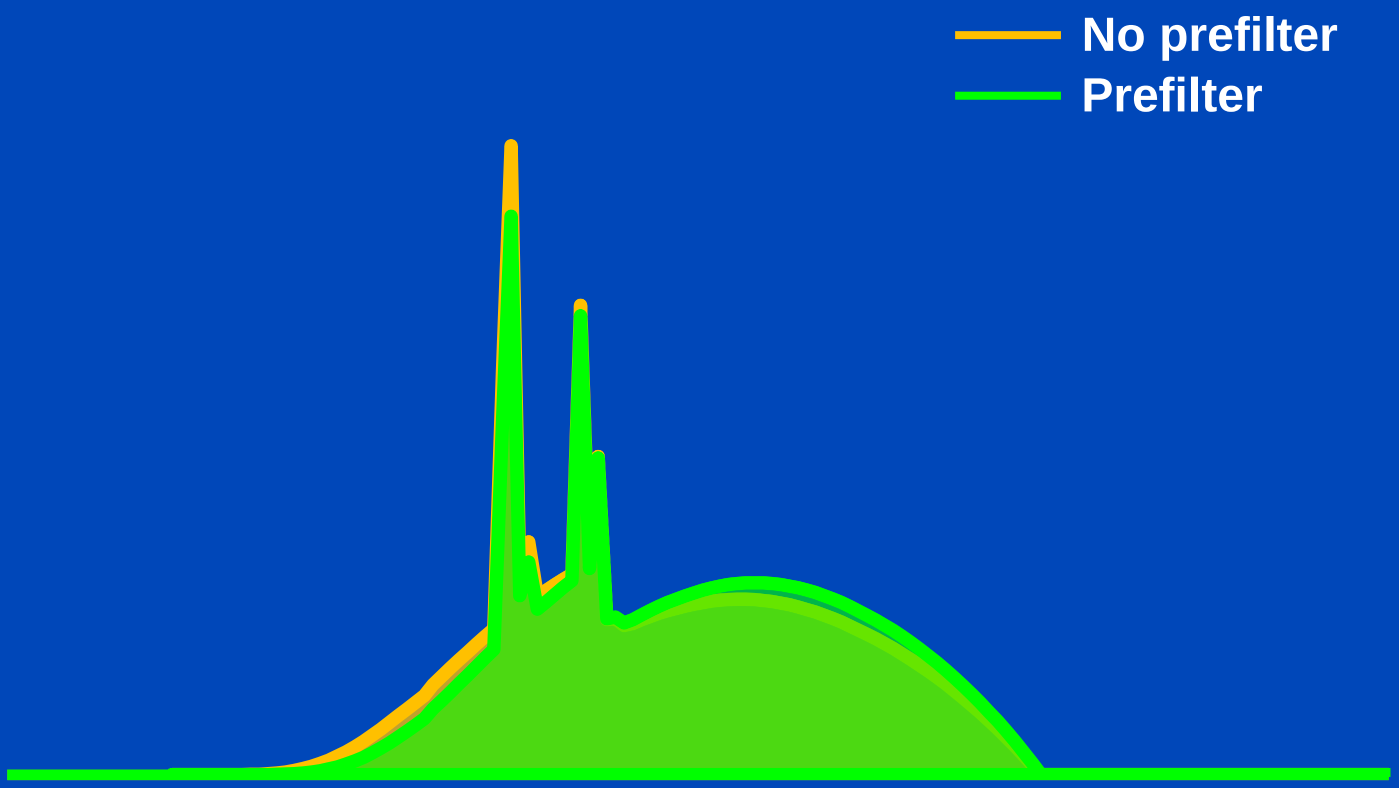

LUNG CANCER SCREENING CT (selected SIEMENS scanners, continued)

(Back to INDEX)

TOPOGRAM: PA; scan from top of shoulder through mid-liver.

SIEMENS	Definition DS (Dual source 64-slice)	Somatom Drive (Dual source 128-slice)	Definition Flash (Dual source 128-slice)	Definition Force (Dual source 192-slice)
Software version	VA44	VB10	VB10	VB10
Scan Mode	Spiral	Spiral	Spiral	Spiral
Rotation Time (s)	0.5	0.5	0.5	0.5
Detector Configuration	*64 × 0.6 mm (32 x 0.6 mm =19.2 mm)	*128 × 0.6 mm (64 x 0.6 mm = 38.4 mm)	*128 × 0.6 mm (64 x 0.6 mm = 38.4 mm)	*192 × 0.6 mm (96 x 0.6 mm = 57.6 mm)
Pitch	1.2	1.2	1.2	1.2
kV	120	100Sn	120	100Sn
Quality ref. mAs	20	81	20	101
CARE Dose4D	ON	ON	ON	ON
CARE kV	ON	ON	ON	ON
CTDIvol***	1.4 mGy	0.6mGy	1.3 mGy	0.4 mGy

RECON 1

Type	Axial	Axial	Axial	Axial
Kernel	B31f	Bf37, strength = 3**	Bf37, strength = 3**	Br40, strength = 3**
Slice (mm)	5.0	5.0	5.0	5.0
Increment (mm)	5.0	5.0	5.0	5.0

dkfz.

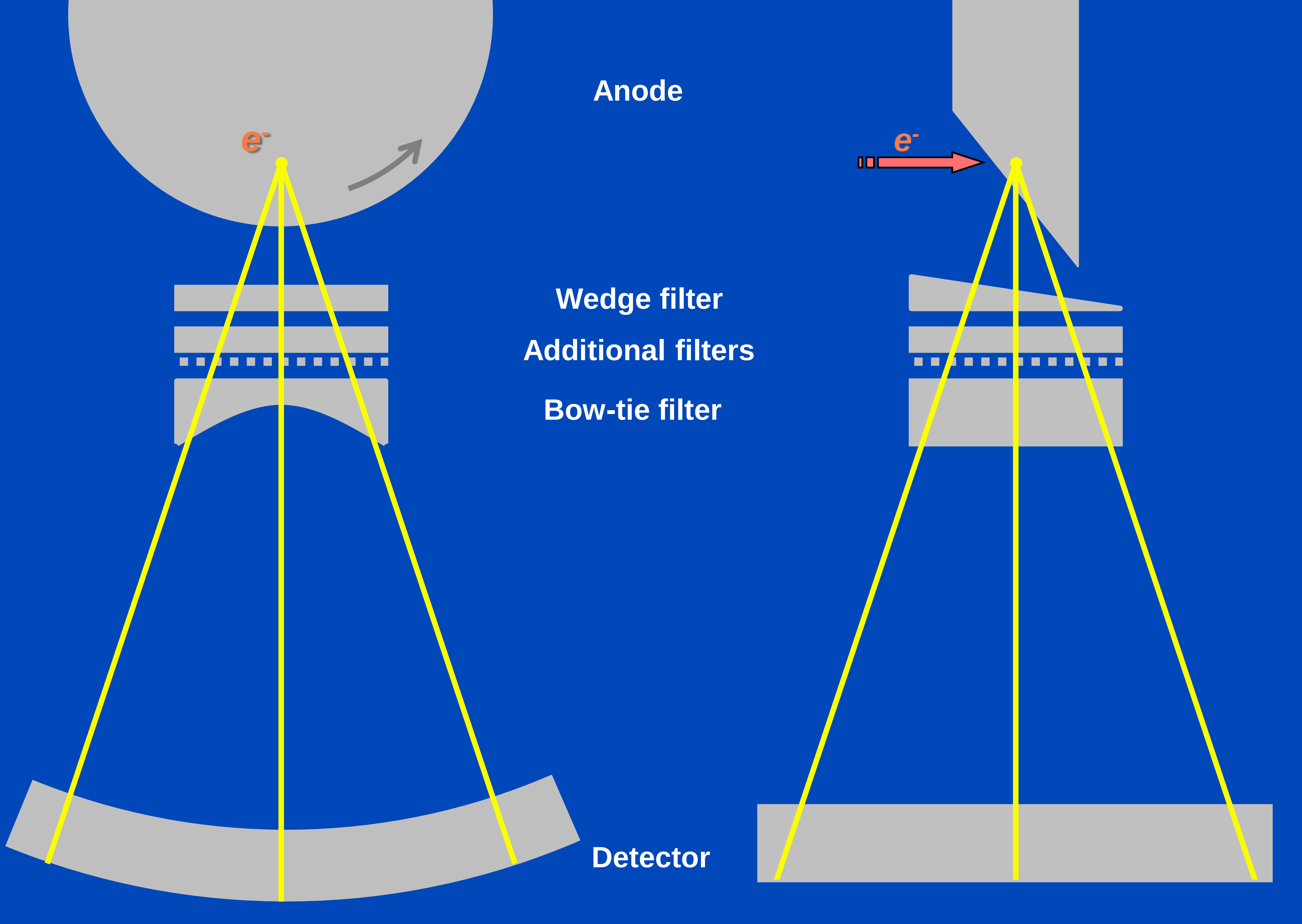

Figure not drawn to scale. Type and order of prefiltration may differ from scanner to scanner.
Depending on the selected protocol filters are changed automatically (e.g. small bowtie for pediatric scans).

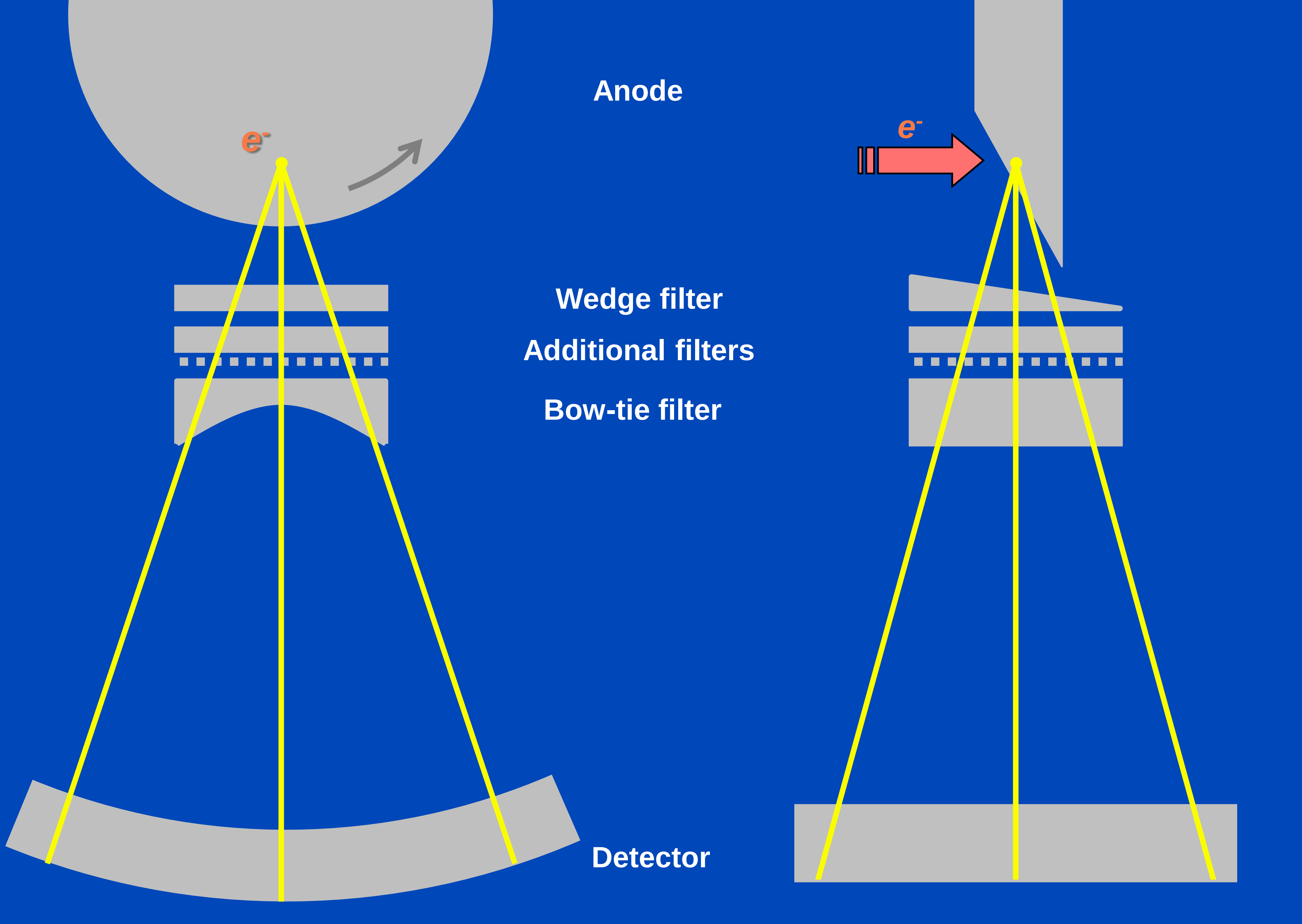

Figure not drawn to scale. Type and order of prefiltration may differ from scanner to scanner.
Depending on the selected protocol filters are changed automatically (e.g. small bowtie for pediatric scans).

Tube Voltage 80 kV

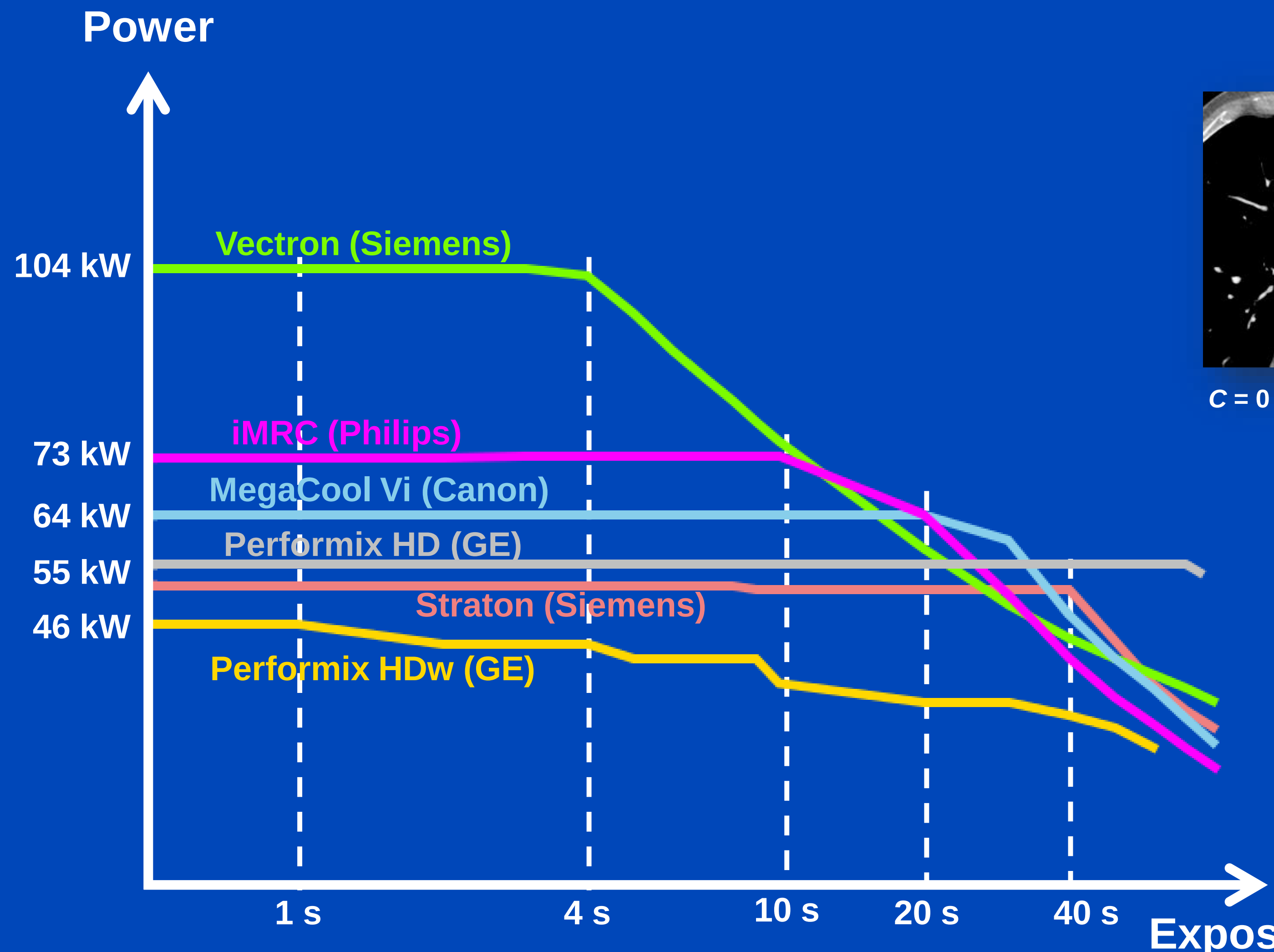

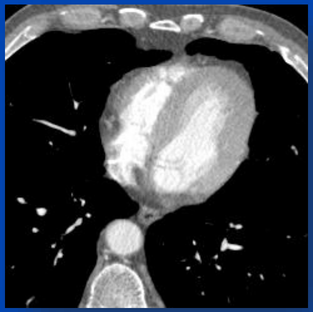

C = 0 HU, *W* = 700 HU

Narrow Cone = High Tube Power

Wide Cone = Low Tube Power

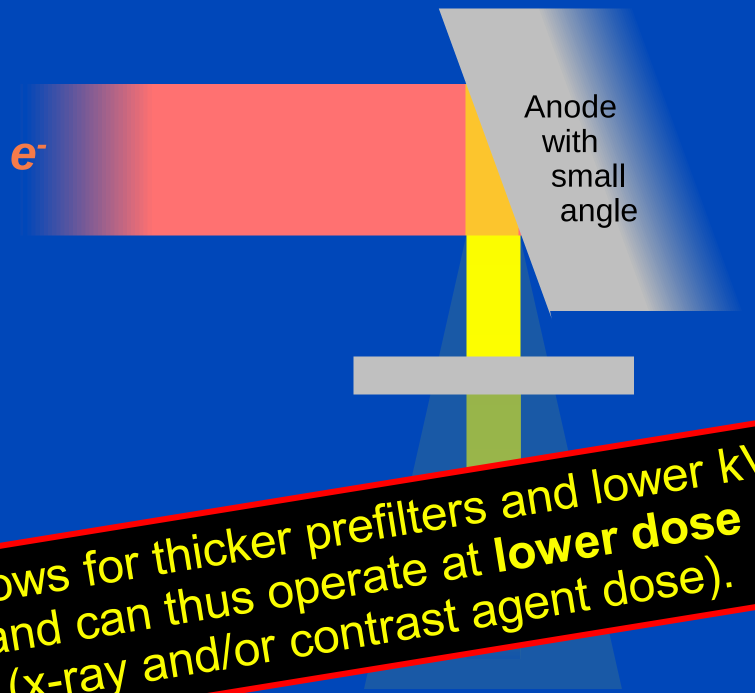

Allows for thicker prefilters and lower kV and can thus operate at **lower dose** (x-ray and/or contrast agent dose).

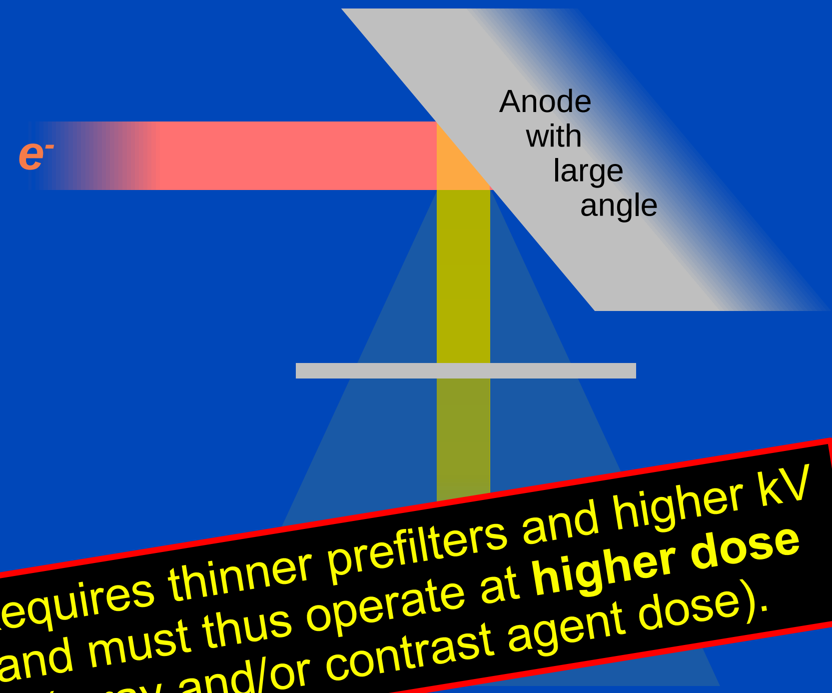

Requires thinner prefilters and higher kV and must thus operate at **higher dose** (x-ray and/or contrast agent dose).

… at the same spatial resolution

Onset of target melting (rule of thumb)[1]: 1 W/µm

[1] D.E. Grider, A. Writh, and P.K. Ausburn. Electron Beam Melting in Microfocus X-Ray Tubes. J. Phys. D: Appl. Phys 19:2281-2292, 1986

Lung Cancer Screening

- From Lung Screening Program at UCLA

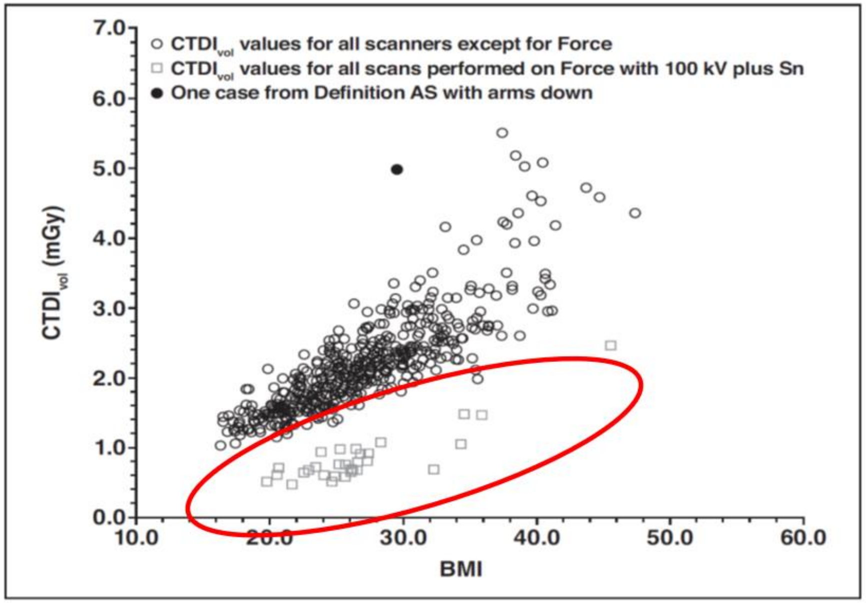

Cases from Force Scanner performed with 100 kV/Sn

~ 40-50% lower dose

David Geffen School of Medicine

UCLA Health

Courtesy of Prof. Michael McNitt Gray, UCLA

dkfz.

European Journal of Radiology 84 (2015) 1608–1613

Contents lists available at ScienceDirect

European Journal of Radiology

journal homepage: www.elsevier.com/locate/ejrad

Unenhanced third-generation dual-source chest CT using a tin filter for spectral shaping at 100 kVp

Holger Haubenreisser[a,*], Mathias Meyer[a], Sonja Sudarski[a], Thomas Allmendinger[b], Stefan O. Schoenberg[a], Thomas Henzler[a]

[a] Institute of Clinical Radiology and Nuclear Medicine, University Medical Center Mannheim, Medical Faculty Mannheim, Heidelberg University, Germany
[b] Siemens Healthcare Sector, CT Division, Forchheim, Germany

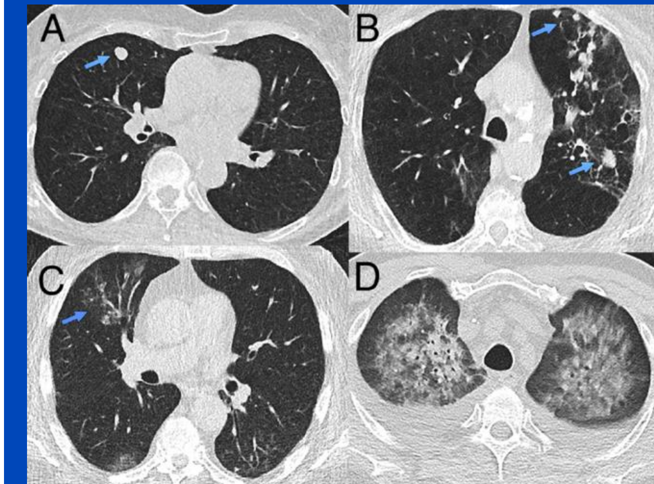

100 kVp with spectral shaping. (A and B) Lung nodules, (C) atypical pneumonia, (D) pneumocystis pneumonia.

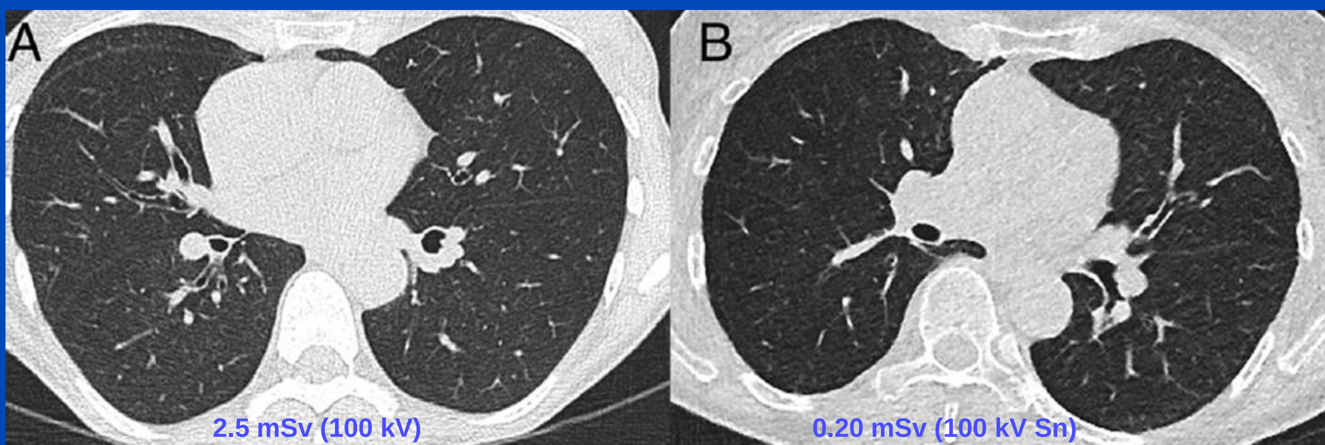

(A) 100 kVp without spectral shaping ($CTDI_{vol}$ 3.8 mGy; DLP 137 mGy cm). (B) 100 kVp with spectral shaping ($CTDI_{vol}$ 0.32 mGy; DLP 11 mGy cm).

All images were reconstructed with a slice thickness of 1.5 mm in the axial and coronal planes using a corresponding lung kernel (3rd generation DSCT: Bl57; 2nd generation DSCT: I70f), with the 3rd generation DSCT utilizing a novel iterative reconstruction technique (Adaptive Model-based Iterative Reconstruction (ADMIRE), Siemens Healthcare, Forchheim, Germany). This algorithm was described in detail in a recent study [9]. The 2nd generation DSCT utilized a previously described iterative reconstruction algorithm (Sinogram Affirmed Iterative Reconstruction (SAFIRE), Siemens Healthcare, Forchheim, Germany). The iterative reconstruction algorithm was set at a level of 3 for all reconstructions. The iteration level of 3 was chosen since the retrospective studies from the 2nd generation DSCT were all performed with a strength level of 3. That strength level resulted in the best image quality based on our experience and was clinically performed in all retrospectively included studies on the 2nd generation DSCT. Further, initial results in a phantom study showed that iterative levels of 3 and 5 yield diagnostically acceptable results [9]. The images were then exported to an offline workstation (Aycan Osirix Pro 2, Aycan, Würzburg, Germany) for all data analysis.

Dosimetric parameters for both protocols.

	Reference mAs	Effective mAs	CTDI (mGy)	DLP (mGy cm)	Equiv. dose (mSv)
Group A	96	167.5 ± 108.0	0.49 ± 0.18	17.7 ± 6.8	0.32 ± 0.12
Group B	96	79 ± 7.0	4.9 ± 1.9	166.9 ± 66.1	3.0 ± 1.2

Dose Reduction by Patient-Specific Tin or Copper Prefilters[1,2] 1000 mAs Limit, 70-150 kV, 10 kV steps

	Child (15 cm × 10 cm) 	**Adult** (30 cm × 20 cm) 	**Obese** (50 cm × 40 cm) 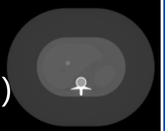
Soft tissue (basis)	30 mAs, 90 kV	100 mAs, 130 kV	600 mAs, 150 kV
Soft tissue, Sn	0.6 mm, 1000 mAs, 80 kV **14%** → 19%	1.0 mm, 1000 mAs, 120 kV **32%** → 36%	0.2 mm, 870 mAs, 150 kV **25%** → 57%
Soft tissue, Cu	1.6 mm, 1000 mAs, 70 kV **17%** → 19%	3.1 mm, 1000 mAs, 120 kV **31%** → 36%	0.8 mm, 1000 mAs, 150 kV **29%** → 57%
Iodine (basis)	50 mAs, 70 kV	120 mAs, 90 kV	720 mAs, 120 kV
Iodine, Sn	0 mm, 50 mAs, 70 kV **0%**	0.1 mm, 1000 mAs, 70 kV **40%**	0.0 mm, 1000 mAs, 110 kV **26%** → 79%
Iodine, Cu	0.1 mm, 58 mAs, 70 kV **3%**	0.4 mm, 1000 mAs, 70 kV **44%**	0.1 mm, 1000 mAs, 110 kV **28%** → 80%

[1] Steidel, Maier, Sawall, Kachelrieß. Tin or Copper Prefilters for Dose Reduction in Diagnostic Single Energy CT? RSNA 2020.
[2] Steidel, Maier, Sawall, Kachelrieß. Dose Reduction through Patient-Specific Prefilters in Diagnostic Single Energy CT. RSNA 2020.

Dose Reduction by Patient-Specific Tin or Copper Prefilters[1,2]
5000 mAs Limit, 70-150 kV, 10 kV steps

	Child (15 cm × 10 cm) 	Adult (30 cm × 20 cm) 	Obese (50 cm × 40 cm) 
Soft tissue (basis)	30 mAs, 90 kV	100 mAs, 130 kV	600 mAs, 150 kV
Soft tissue, Sn	0.8 mm, 5000 mAs, 70 kV **16%** → 19%	1.6 mm, 5000 mAs, 110 kV **34%** → 36%	1.7 mm, 5000 mAs, 150 kV **50%** → 57%
Soft tissue, Cu	2.5 mm, 5000 mAs, 70 kV **18%** → 19%	5.2 mm, 5000 mAs, 110 kV **33%** → 36%	4.7 mm, 5000 mAs, 150 kV **47%** → 57%
Iodine (basis)	50 mAs, 70 kV	120 mAs, 90 kV	720 mAs, 120 kV
Iodine, Sn	0 mm, 50 mAs, 70 kV **0%**	0.1 mm, 1000 mAs, 70 kV **40%**	0.1 mm, 5000 mAs, 80 kV **67%** → 79%
Iodine, Cu	0.1 mm, 58 mAs, 70 kV **3%**	0.7 mm, 1600 mAs, 70 kV **44%**	0.2 mm, 5000 mAs, 80 kV **70%** → 80%

[1]Steidel, Maier, Sawall, Kachelrieß. Tin or Copper Prefilters for Dose Reduction in Diagnostic Single Energy CT? RSNA 2020.
[2]Steidel, Maier, Sawall, Kachelrieß. Dose Reduction through Patient-Specific Prefilters in Diagnostic Single Energy CT. RSNA 2020.

Dose Reduction by Patient-Specific Tin or Copper Prefilters[1,2] 5000 mAs Limit

	Child (15 cm × 10 cm) 	Adult (30 cm × 20 cm) 	Obese (50 cm × 40 cm) 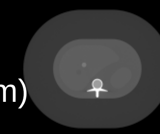
Soft tissue (basis)	30 mAs, 90 kV	100 mAs, 130 kV	600 mAs, 150 kV
Soft tissue, Sn	0.8 mm, 5000 mAs, 70 kV **16%** → 19%	1.4 mm, 5000 mAs, 105 kV **35%** → 36%	1.7 mm, 5000 mAs, 150 kV **50%** → 57%
Soft tissue, Cu	2.2 mm, 5000 mAs, 65 kV **18%** → 19%	4.3 mm, 5000 mAs, 105 kV **34%** → 36%	4.7 mm, 5000 mAs, 150 kV **47%** → 57%
Iodine (basis)	50 mAs, 70 kV	120 mAs, 90 kV	720 mAs, 120 kV
Iodine, Sn	0 mm, 210 mAs, 50 kV **39%**	0.2 mm, 5000 mAs, 60 kV **51%** → 53%	0.1 mm, 5000 mAs, 85 kV **67%** → 81%
Iodine, Cu	0.5 mm, 5000 mAs, 45 kV **59%** → 67%	0.6 mm, 5000 mAs, 60 kV **57%** → 68%	0.2 mm, 5000 mAs, 80 kV **70%** → 89%

[1]Steidel, Maier, Sawall, Kachelrieß. Tin or Copper Prefilters for Dose Reduction in Diagnostic Single Energy CT? RSNA 2020.
[2]Steidel, Maier, Sawall, Kachelrieß. Dose Reduction through Patient-Specific Prefilters in Diagnostic Single Energy CT. RSNA 2020.

dkfz.

Prefilters

- **We want**
  - a filter changer with, say, 10 different filters, or a sliding double wedge
  - tubes with much higher power and lower kV
  - to always operate the tube close to its power limit
  - to adjust the filter thickness and kV to the patient
  - copper instead of tin

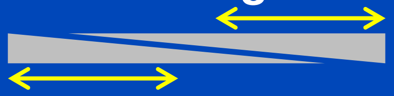

- **We get**
  - a significant dose reduction
  - improved image quality

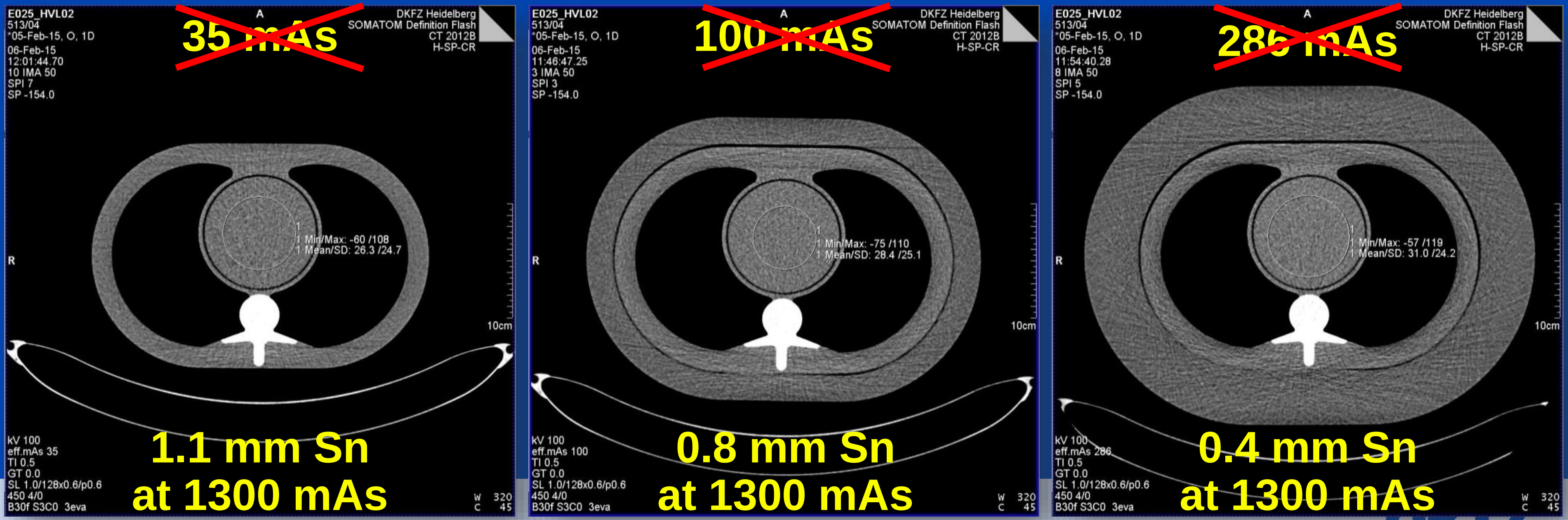

Photon Counting

Photon counting (here: Dectris detector), C/W=1 cnts/2 cnts

X-rays are off!

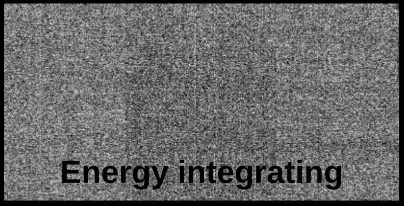

Indirect Conversion (Today) | Direct Conversion (Future)

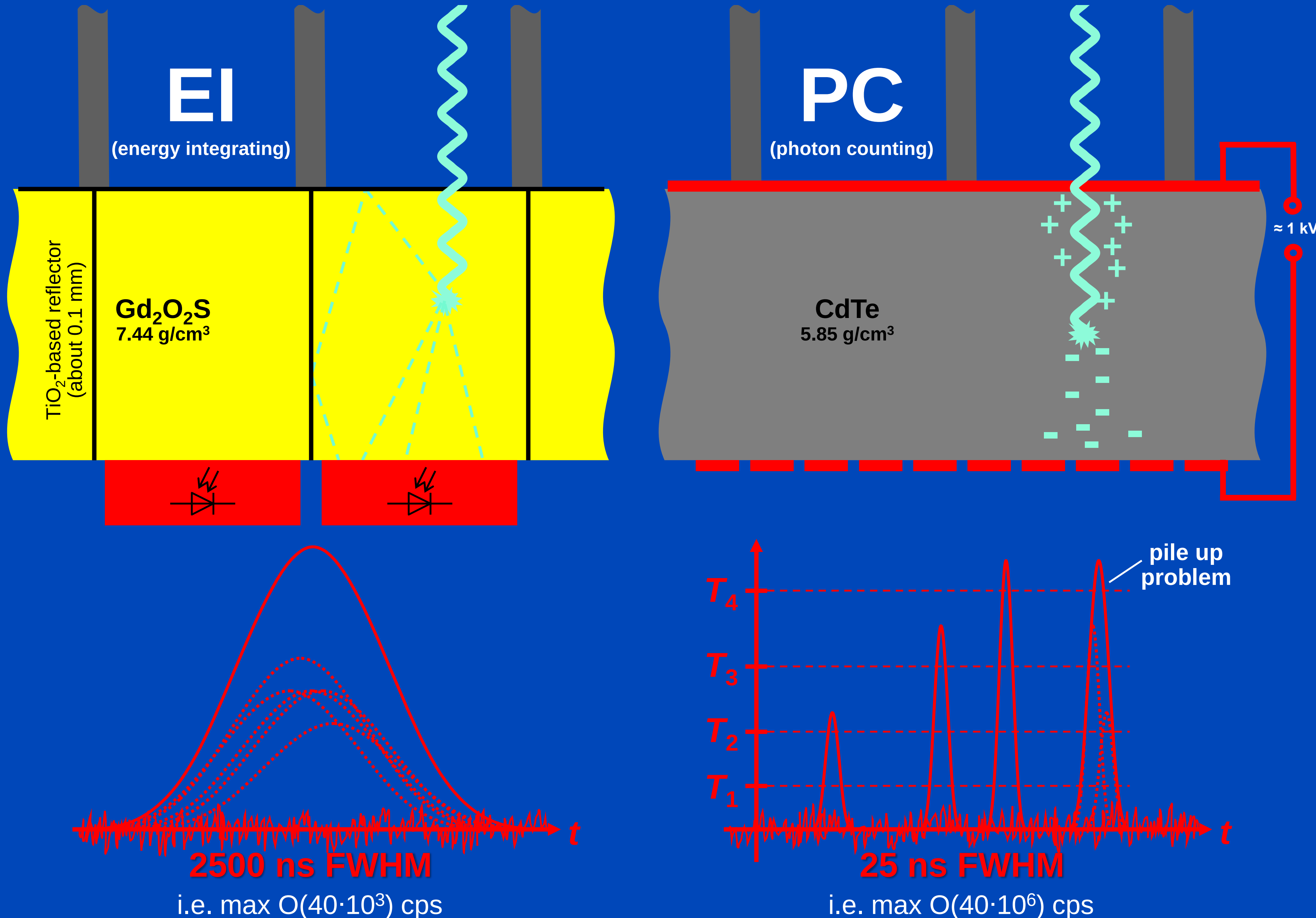

Requirements for CT: up to 10^9 x-ray photon counts per second per mm^2.
Hence, photon counting only achievable for direct converters.

dkfz.

Ideally, bin spectra do not overlap, …

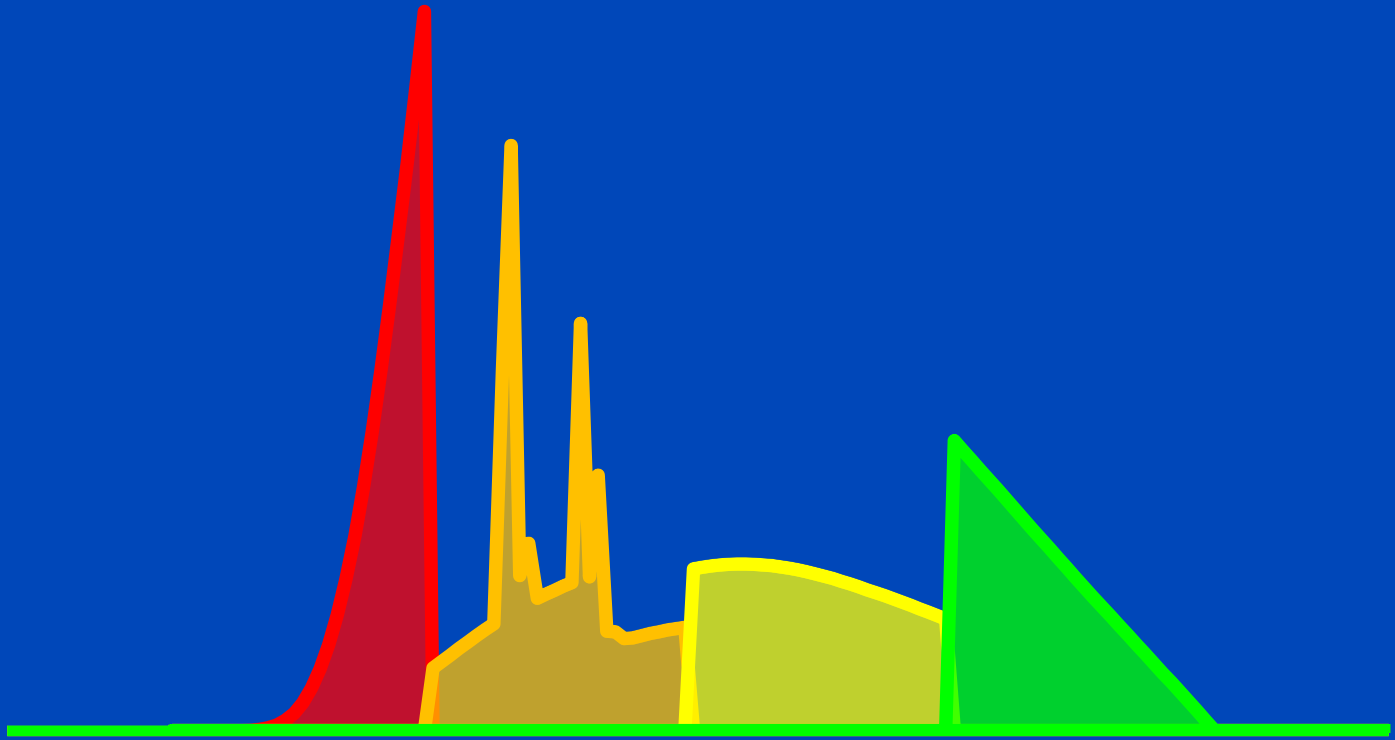

Spectra as seen after having passed a 32 cm water layer.

… realistically, however they do!

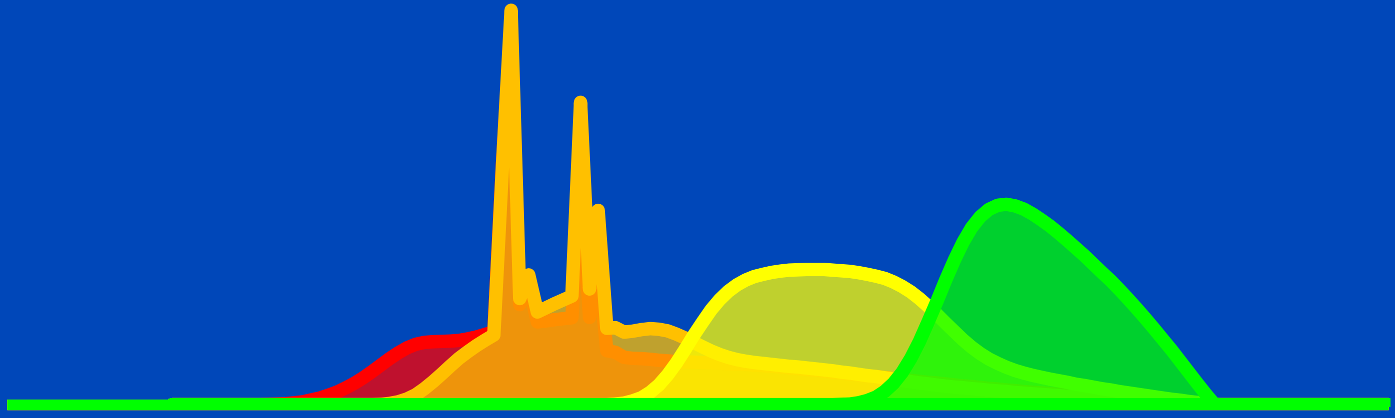

Spectra as seen after having passed a 32 cm water layer.


SIEMENS
SOMATOM CounT
@ dkfz.

Siemens CounT CT System

Gantry from a clinical dual source scanner

A: conventional CT detector (50.0 cm FOV)

B: Photon counting detector (27.5 cm FOV)

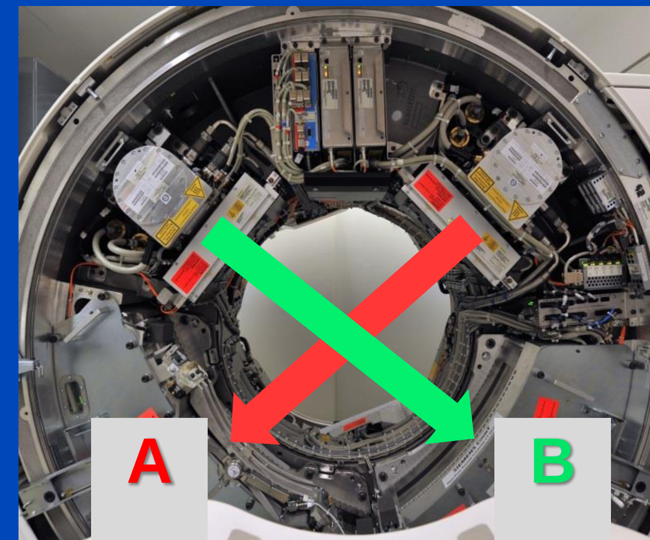

Readout Modes of the CounT

PC-UHR Mode	PC-Macro Mode	EI detector
0.25 mm pixel size	0.50 mm pixel size	0.60 mm pixel size

Experimental CT, not commercially available.

Advantages of Photon Counting CT

- No reflective gaps between detector pixels
  - Higher geometrical efficiency
  - Less dose
- No electronic noise
  - Less dose for infants
  - Less noise for obese patients
- Counting
  - Swank factor = 1 = maximal
  - “Iodine effect“ due to higher weights on low energies
- Energy bin weighting
  - Lower dose/noise
  - Improved iodine CNR
- Smaller pixels (to avoid pileup)
  - Higher spatial resolution
  - “Small pixel effect” i.e. lower dose/noise at conventional resolution
- Spectral information on demand

Photon Counting used to Maximize CNR

- With PC energy bins can be weighted individually.
- To optimize the CNR the optimal bin weighting factor is given by (weighting after log):

$$w_b \propto \frac{C_b}{V_b}$$

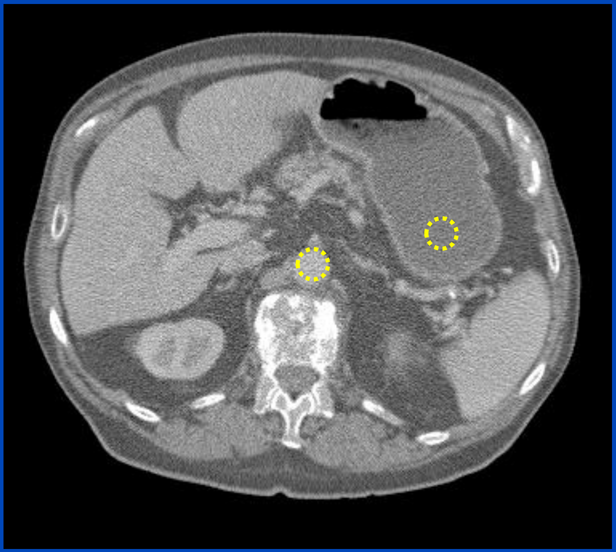

- The resulting CNR is

$$\mathrm{CNR}^2 = \frac{(\sum_b w_b C_b)^2}{\sum_b w_b^2 V_b}$$

- At the optimum this evaluates to

$$\mathrm{CNR}^2 = \sum_{b=1}^{B} \mathrm{CNR}_b^2$$

Energy Integrating vs. Photon Counting
with 4 bins from 20 to 140 keV

Energy Integrating

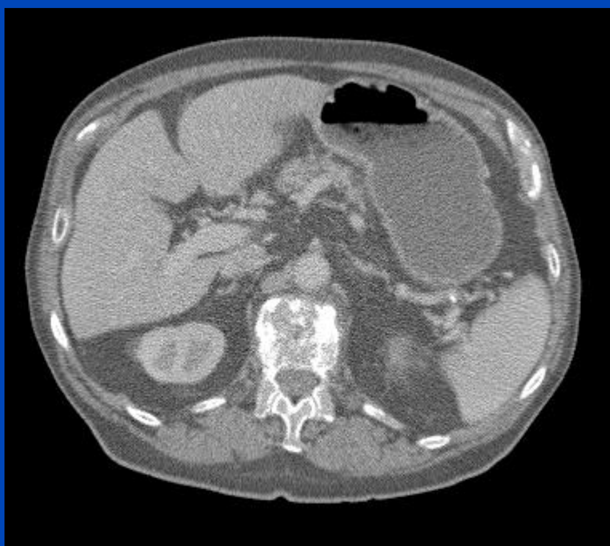

PC minus EI

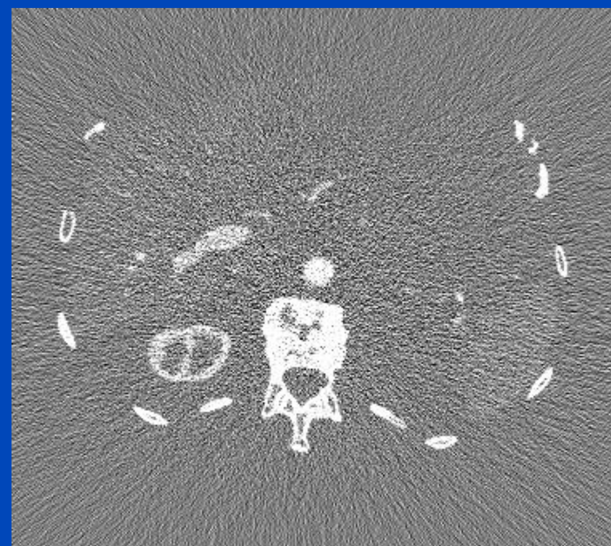

Photon Counting

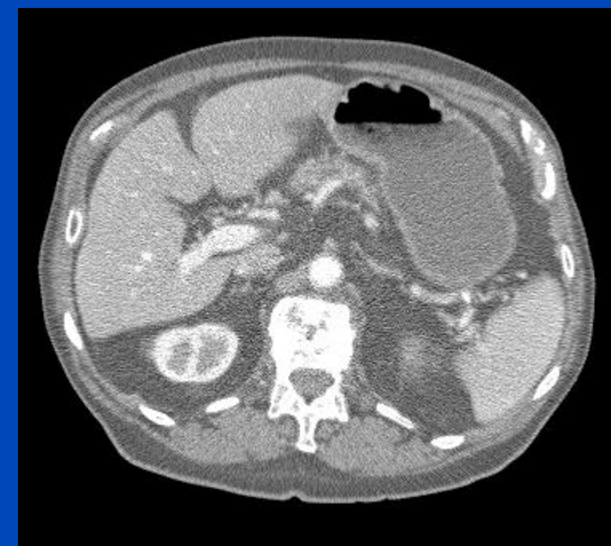

CNR = 2.11

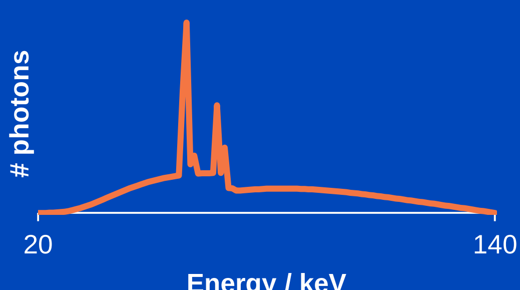

99% CNR improvement or 75% dose reduction achievable due to improved Swank factor and optimized energy weighting.

CNR = 4.19

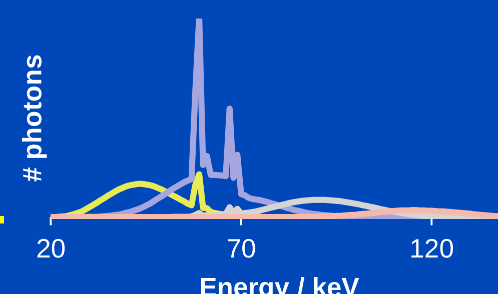

Images: *C* = 0 HU, *W* = 700 HU, difference image: *C* = 0 HU, *W* = 350 HU, bins start at 20 keV

The “Small Pixel Effect”

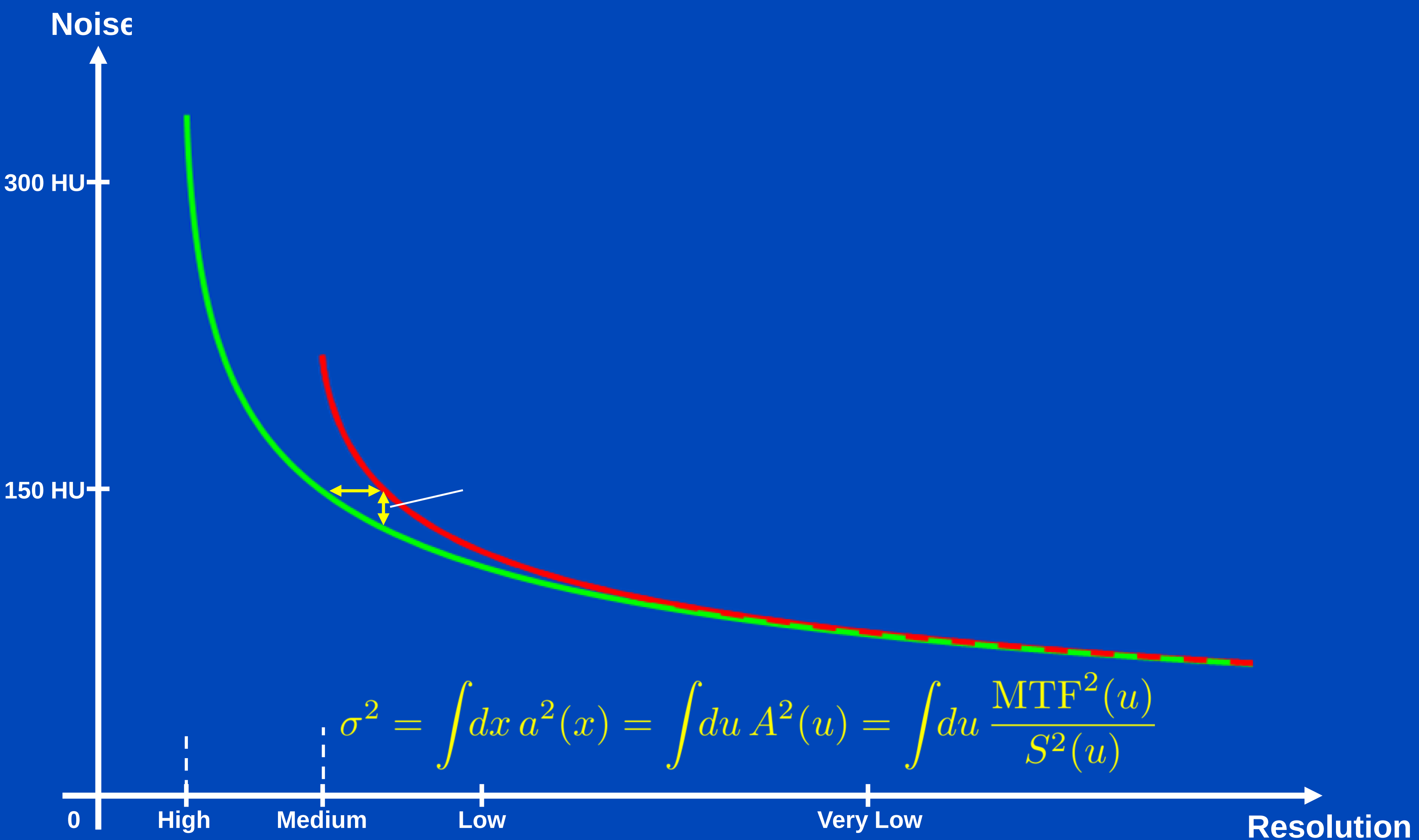

$$\sigma^2 = \int dx\, a^2(x) = \int du\, A^2(u) = \int du\, \frac{\mathrm{MTF}^2(u)}{S^2(u)}$$

Kachelrieß, Kalender. Med. Phys. 32(5):1321-1334, May 2005

All images reconstructed with 1024^2 matrix and 0.15 mm slice increment.
C = 1000 HU
W = 3500 HU

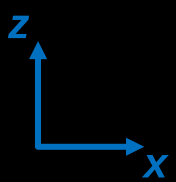

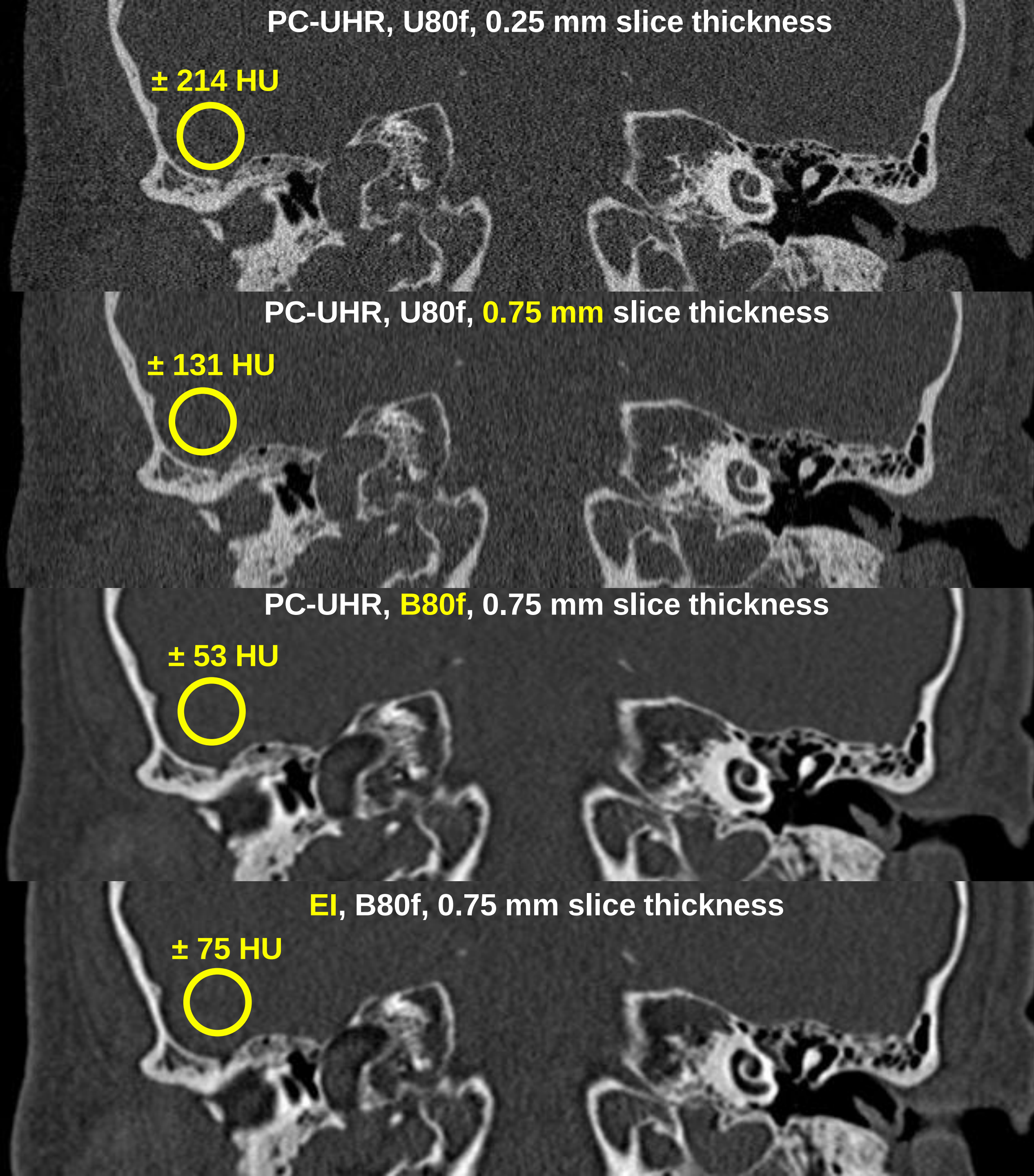

10% MTF: 19.1 lp/cm
10% MTF:17.2 lp/cm
xy FWHM: 0.48 mm
z FWHM: 0.40 mm
$CTDI_{vol}$: 16.0 mGy

10% MTF: 19.1 lp/cm
10% MTF:17.2 lp/cm
xy FWHM: 0.48 mm
z FWHM: 0.67 mm
$CTDI_{vol}$: 16.0 mGy

10% MTF: 9.3 lp/cm
10% MTF:10.5 lp/cm
xy FWHM: 0.71 mm
z FWHM: 0.67 mm
$CTDI_{vol}$: 16.0 mGy

10% MTF: 9.3 lp/cm
10% MTF:10.5 lp/cm
xy FWHM: 0.71 mm
z FWHM: 0.67 mm
$CTDI_{vol}$: 16.0 mGy

Data courtesy of the Institute of Forensic Medicine of the University of Heidelberg and of the Division of Radiology of the German Cancer Research Center (DKFZ)

L. Klein, C. Amato, S. Heinze, M. Uhrig, H.-P. Schlemmer, M. Kachelrieß, and S. Sawall. **Effects of Detector Sampling on Noise Reduction in a Clinical Photon Counting Whole-Body CT**. Investigative Radiology, vol. 55(2), in press, February 2020.

Energy Integrating Detector (B70f)

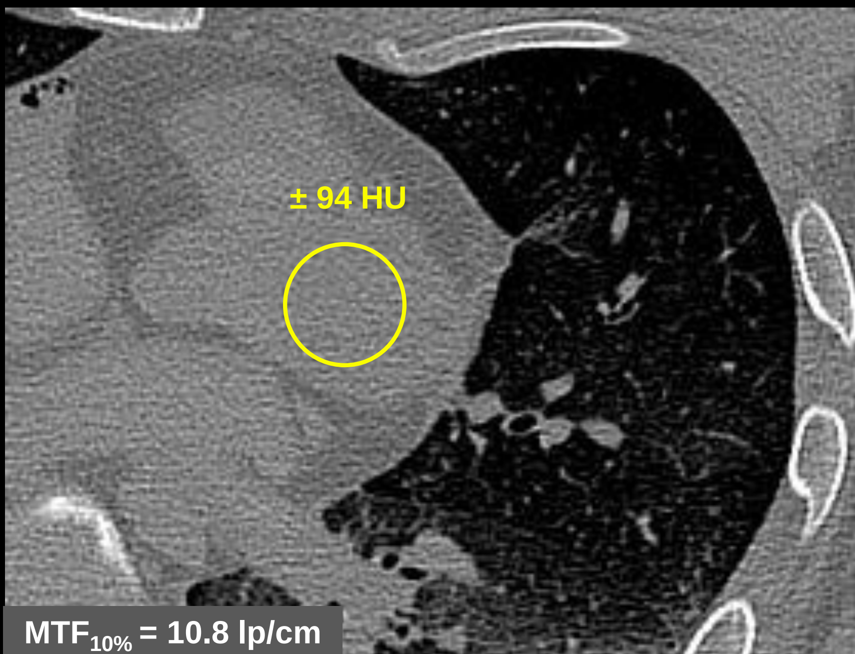

Photon Counting Detector (B70f)

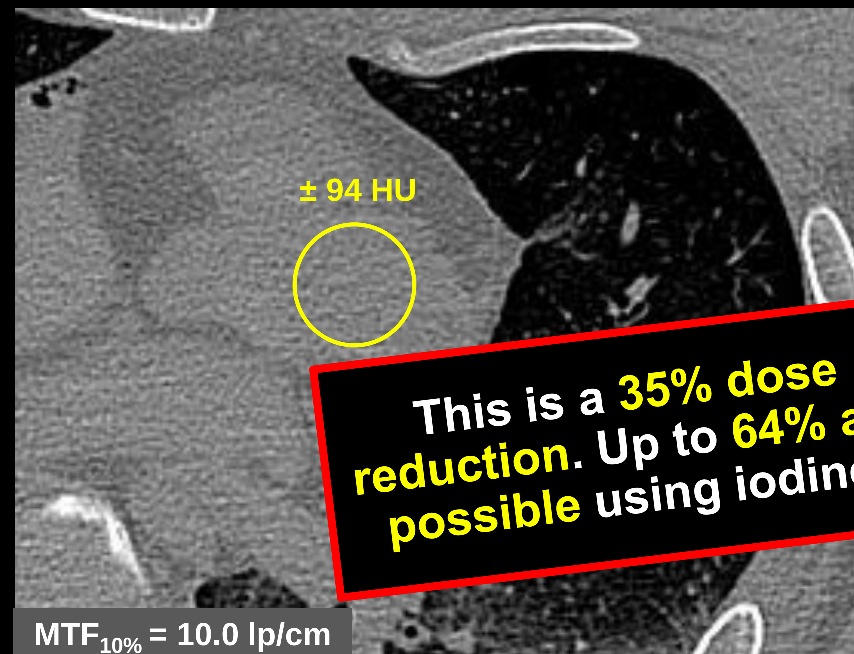

Acquisition with EI:
- Tube voltage of 120 kV
- Tube current of 300 mAs
- Resulting dose of CTDI$_{\text{vol 32 cm}}$ = 22.6 mGy

Acquisition with UHR:
- Tube voltage of 120 kV
- Tube current of 180 mAs
- Resulting dose of CTDI$_{\text{vol 32 cm}}$ = 14.6 mGy

C = 50 HU, W = 1500 HU

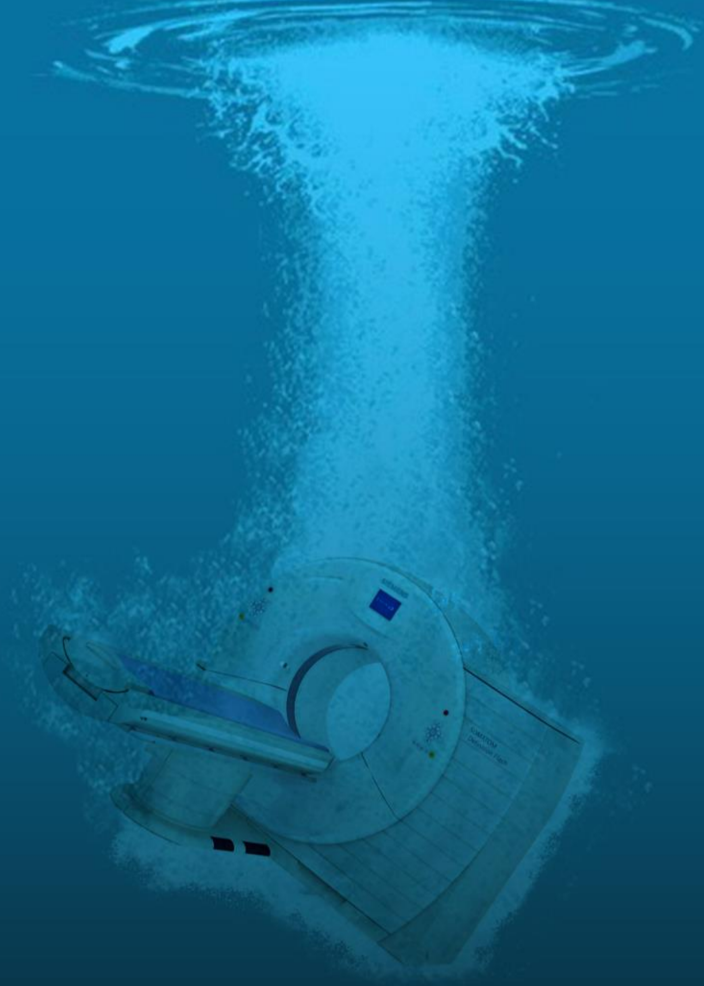

Deep Learning

Metal Artifact Reduction Example

- Deep CNN-driven patch-based combination of the advantages of several MAR methods trained on simulated artifacts

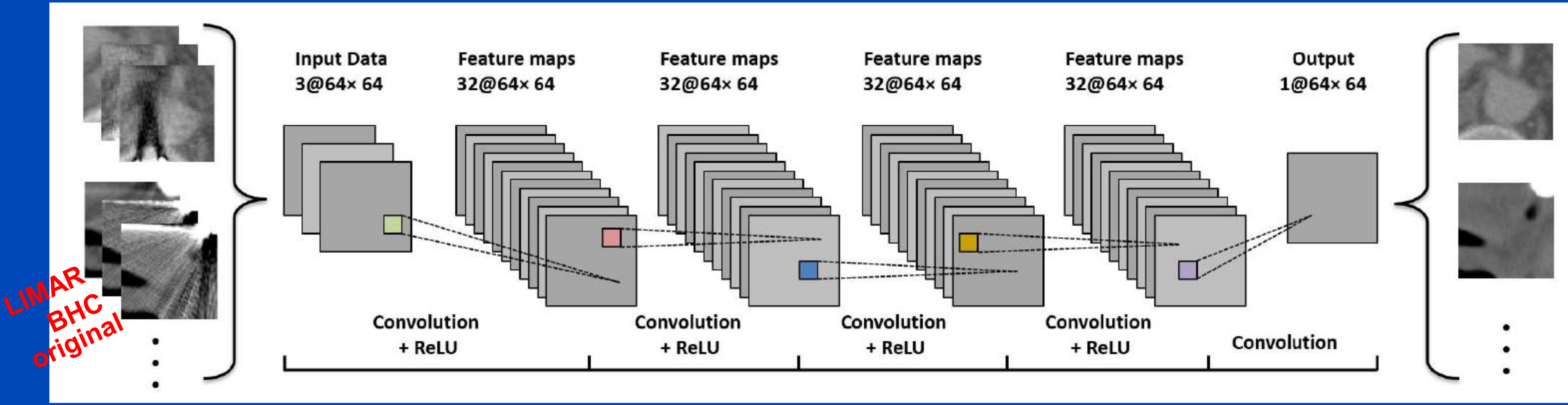

- followed by segmentation into tissue classes
- followed by forward projection of the CNN prior and replacement of metal areas of the original sinogram
- followed by reconstruction

Yanbo Zhang and Hengyong Yu. Convolutional Neural Network Based Metal Artifact Reduction in X-Ray Computed Tomography. TMI 37(6):1370-1381, June 2018.

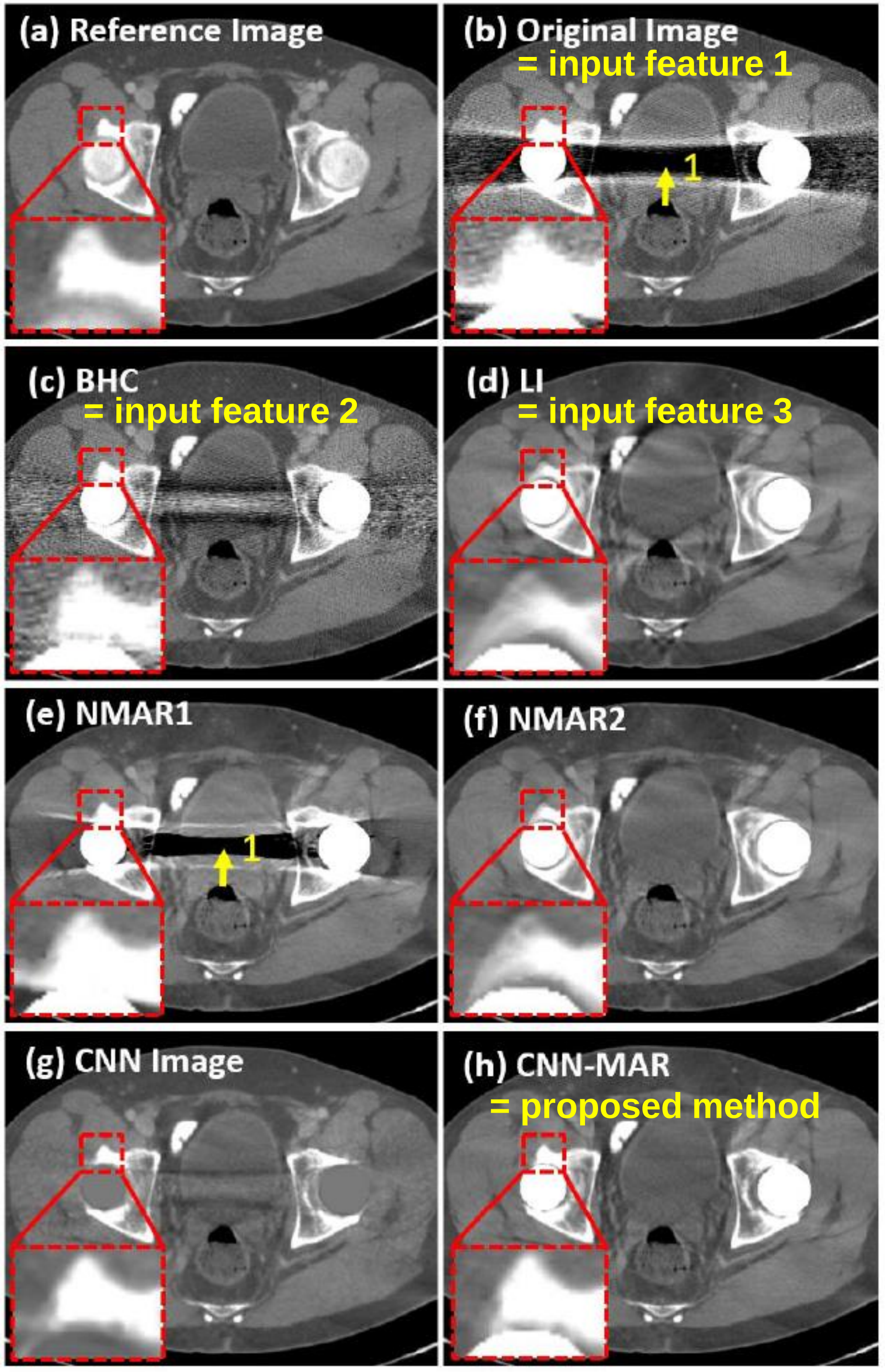
(a) Reference Image
(b) Original Image
= input feature 1
1
(c) BHC
= input feature 2
(d) LI
= input feature 3
(e) NMAR1
1
(f) NMAR2
(g) CNN Image
(h) CNN-MAR
= proposed method

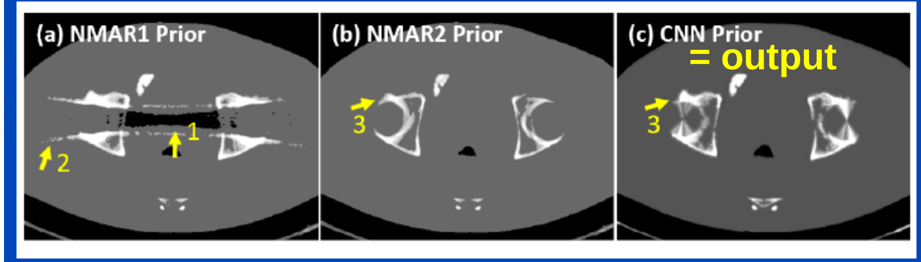
(a) NMAR1 Prior
1
2
(b) NMAR2 Prior
3
(c) CNN Prior
= output
3

Generative Adversarial Network[1] (GAN)

- Useful, if no direct ground truth (GT) is available, the training data are unpaired, unsupervised learning

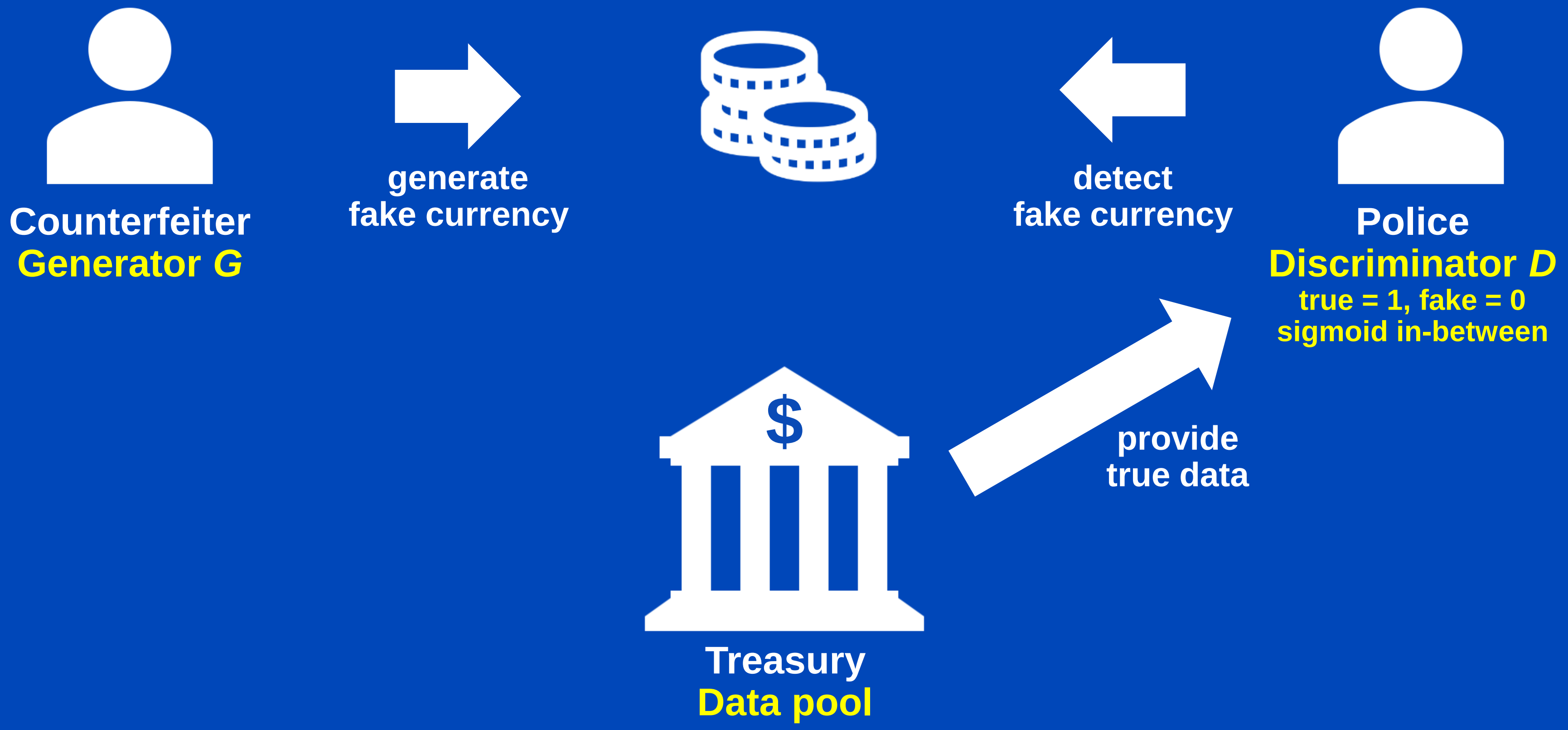

Noise Removal Example

- Task: Reduce noise from low dose CT images.
- A conditional generative adversarial networks (GAN) is used
- Generator *G*:
  - 3D CNN that operates on small cardiac CT sub volumes
  - Seven 3×3×3 convolutional layers yielding a receptive field of 15×15×15 voxels for each destination voxel
  - Depths (features) from 32 to 128
  - Batch norm only in the hidden layers
  - Subtracting skip connection
- Discriminator *D*:
  - Sees either routine dose image or a generator-denoised low dose image
  - Two 3×3×3 layers followed by several 3×3 layers with varying strides
  - Feedback from *D* prevents smoothing.
- Training:
  - Unenhanced (why?) patient data acquired with Philips Briliance iCT 256 at 120 kV.
  - Two scans (why?) per patient, one with 0.2 mSv and one with 0.9 mSv effective dose.

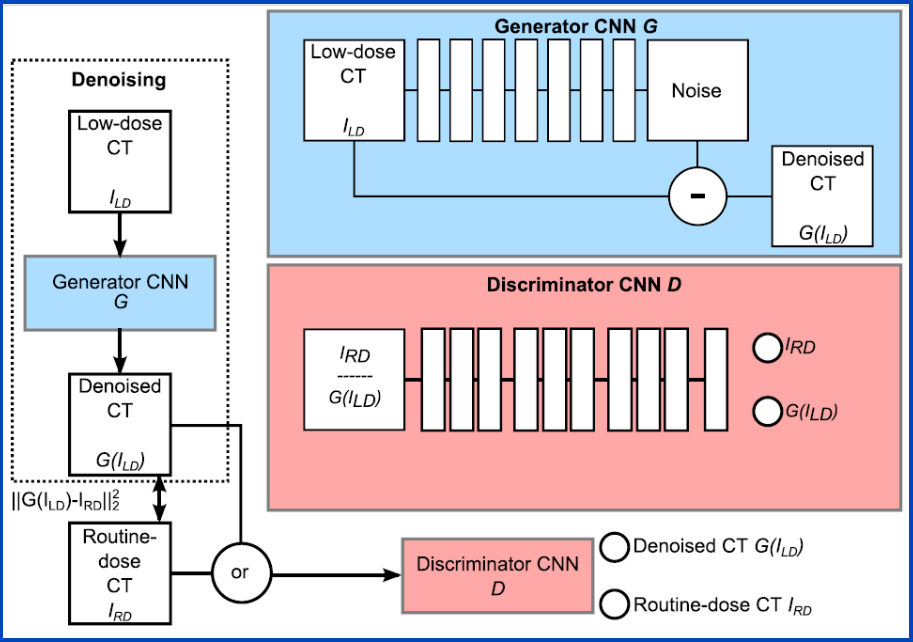

J. Wolterink, T. Leiner, M. Viergever, and I. Išgum. Generative Adversarial Networks for Noise Reduction in Low-Dose CT. IEEE TMI 36(12):2536-2544, Dec. 2017.

Noise Removal Example

Low dose image (0.2 mSv)

J. Wolterink, T. Leiner, M. Viergever, and I. Išgum. Generative Adversarial Networks for Noise Reduction in Low-Dose CT. IEEE TMI 36(12):2536-2544, Dec. 2017.

Noise Removal Example

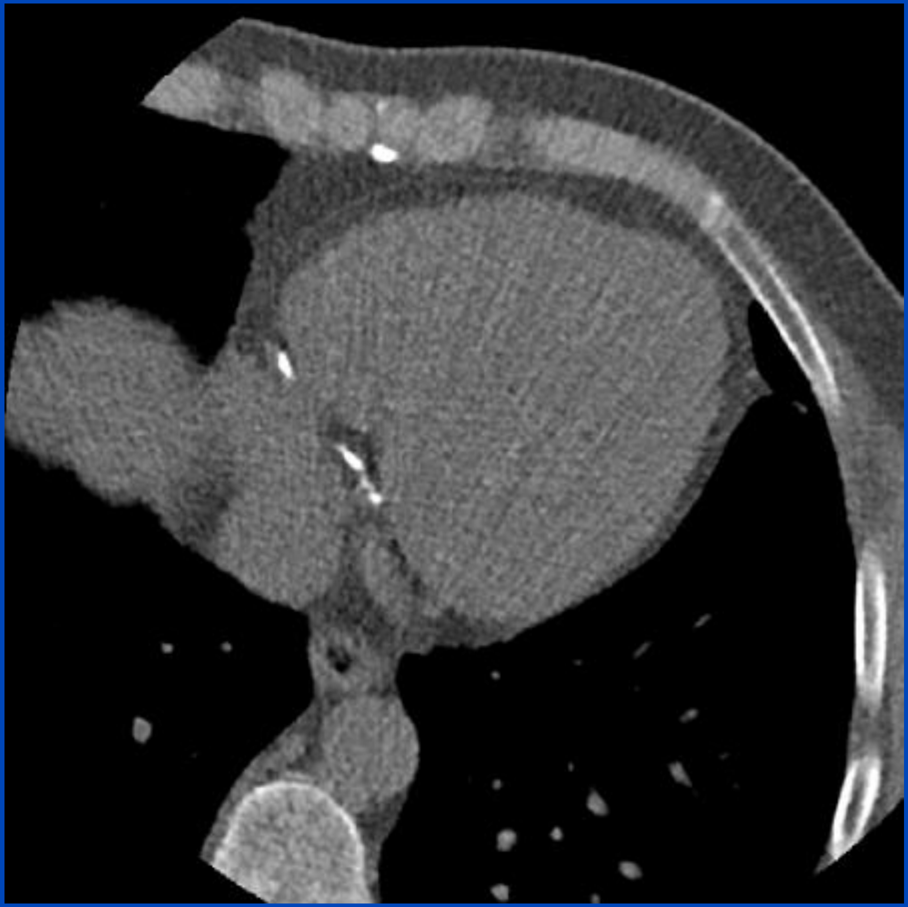

iDose level 3 reconstruction (0.2 mSv)

J. Wolterink, T. Leiner, M. Viergever, and I. Išgum. Generative Adversarial Networks for Noise Reduction in Low-Dose CT. IEEE TMI 36(12):2536-2544, Dec. 2017.

Noise Removal Example

Denoised low dose image (0.2 mSv)

J. Wolterink, T. Leiner, M. Viergever, and I. Išgum. Generative Adversarial Networks for Noise Reduction in Low-Dose CT. IEEE TMI 36(12):2536-2544, Dec. 2017.

Noise Removal Example

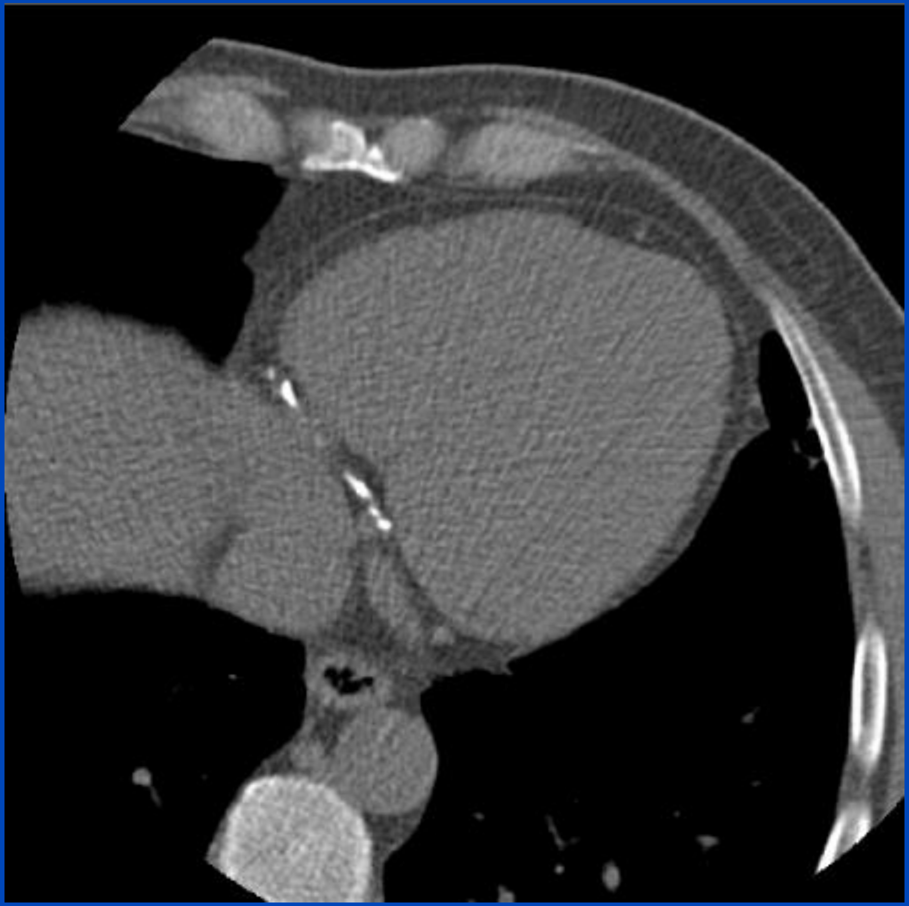

Normal dose image (0.9 mSv)

J. Wolterink, T. Leiner, M. Viergever, and I. Išgum. Generative Adversarial Networks for Noise Reduction in Low-Dose CT. IEEE TMI 36(12):2536-2544, Dec. 2017.

Canon's AiCE

- **Advanced intelligent Clear-IQ Engine (AiCE)**
- **Trained to restore low-dose CT data to match the properties of FIRST, the model-based IR of Canon.**
- **FIRST is applied to high-dose CT images to obtain a high fidelity training target**

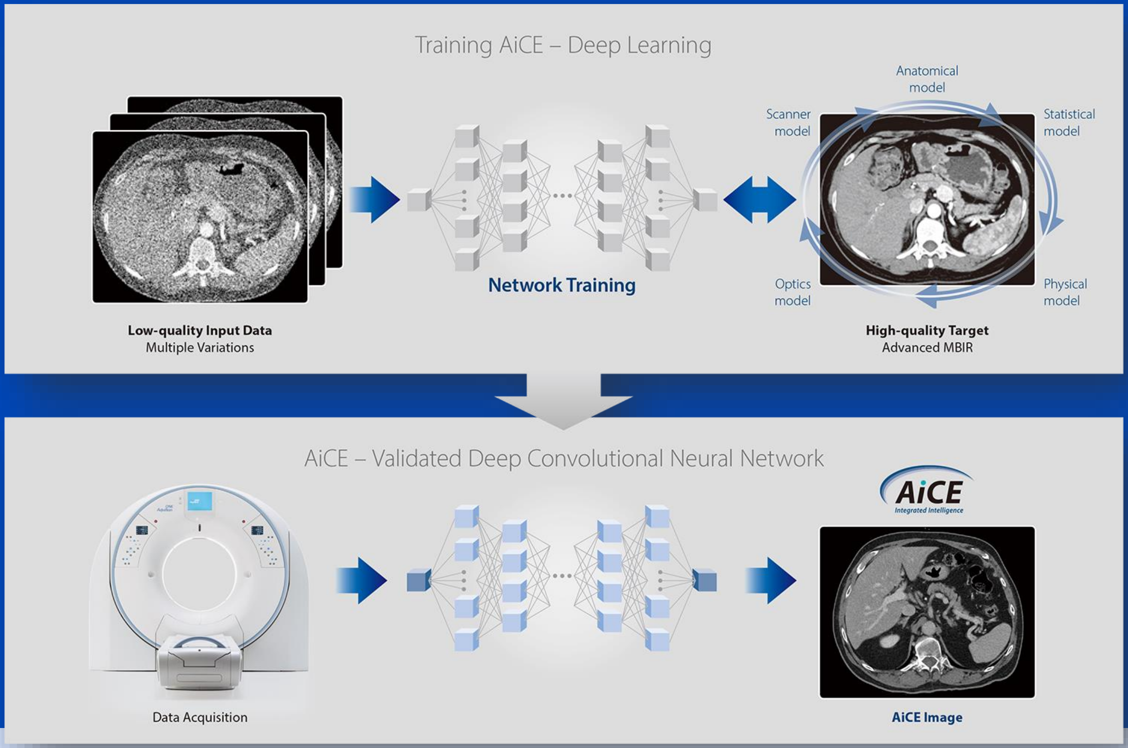

U = 100 kV
CTDI = 0.6 mGy
DLP = 24.7 mGy·cm
D_{eff} = 0.35 mSv

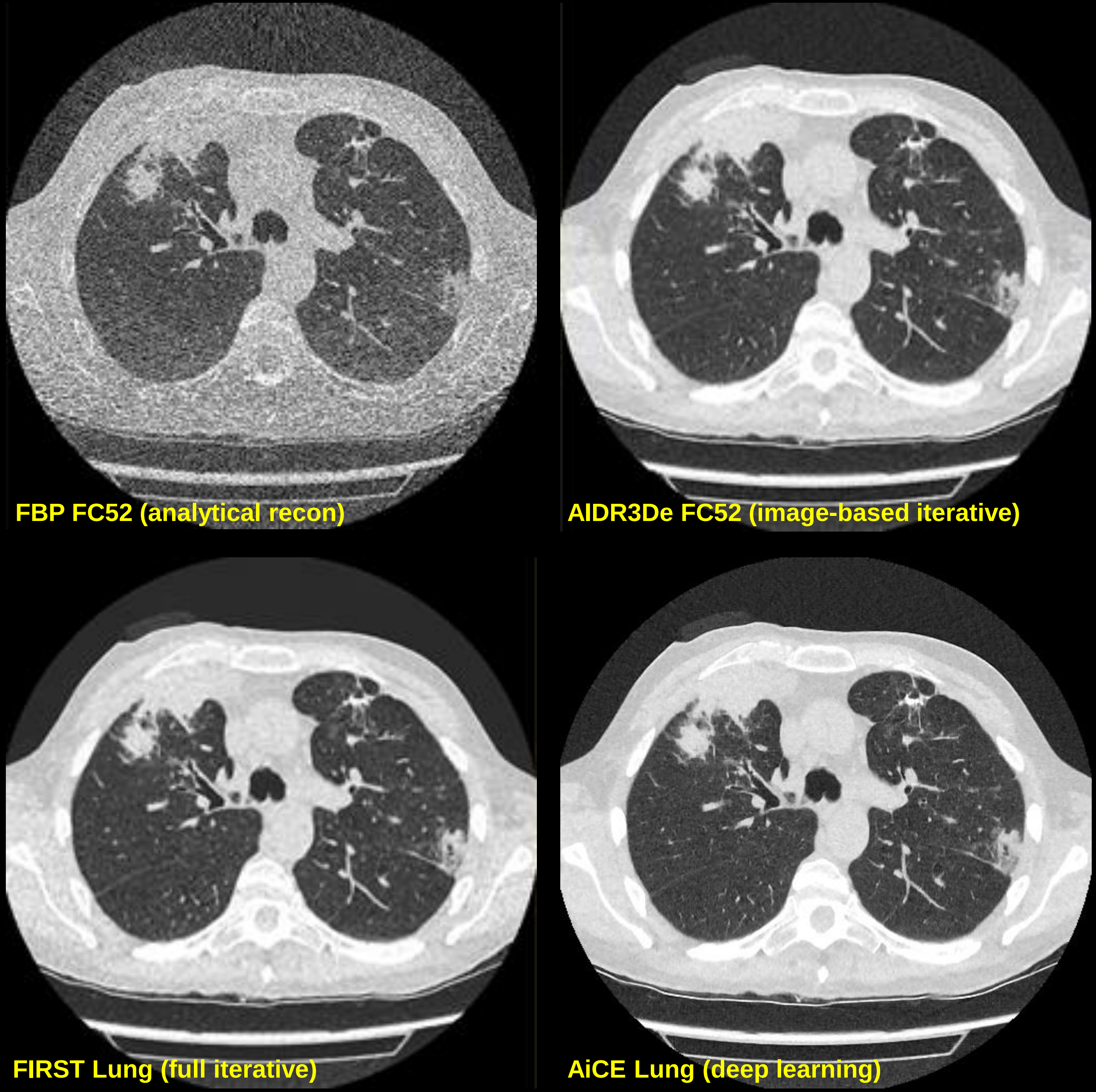

Courtesy of
Radboudumc,
the Netherlands

GE's True Fidelity

- Trained to restore low-dose CT data to match the properties of Veo, the model-based IR of GE.
- No information can be obtained in how the training is conducted for the product implementation.

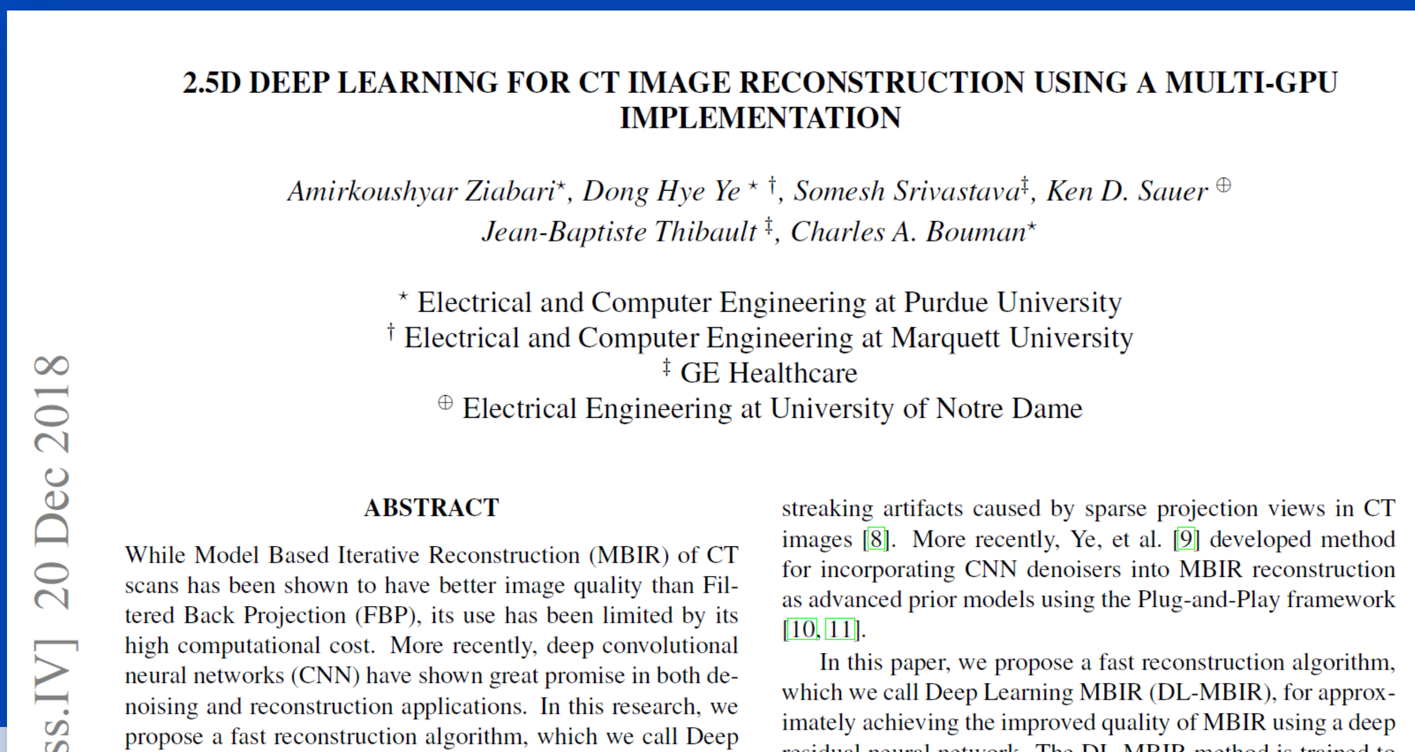

2.5D DEEP LEARNING FOR CT IMAGE RECONSTRUCTION USING A MULTI-GPU IMPLEMENTATION

Amirkoushyar Ziabari[⋆], *Dong Hye Ye*[⋆ †], *Somesh Srivastava*[‡], *Ken D. Sauer*[⊕]
Jean-Baptiste Thibault[‡], *Charles A. Bouman*[⋆]

[⋆] Electrical and Computer Engineering at Purdue University
[†] Electrical and Computer Engineering at Marquett University
[‡] GE Healthcare
[⊕] Electrical Engineering at University of Notre Dame

ABSTRACT

While Model Based Iterative Reconstruction (MBIR) of CT scans has been shown to have better image quality than Filtered Back Projection (FBP), its use has been limited by its high computational cost. More recently, deep convolutional neural networks (CNN) have shown great promise in both denoising and reconstruction applications. In this research, we propose a fast reconstruction algorithm, which we call Deep

streaking artifacts caused by sparse projection views in CT images [8]. More recently, Ye, et al. [9] developed method for incorporating CNN denoisers into MBIR reconstruction as advanced prior models using the Plug-and-Play framework [10, 11].

In this paper, we propose a fast reconstruction algorithm, which we call Deep Learning MBIR (DL-MBIR), for approximately achieving the improved quality of MBIR using a deep residual neural network. The DL-MBIR method is trained to

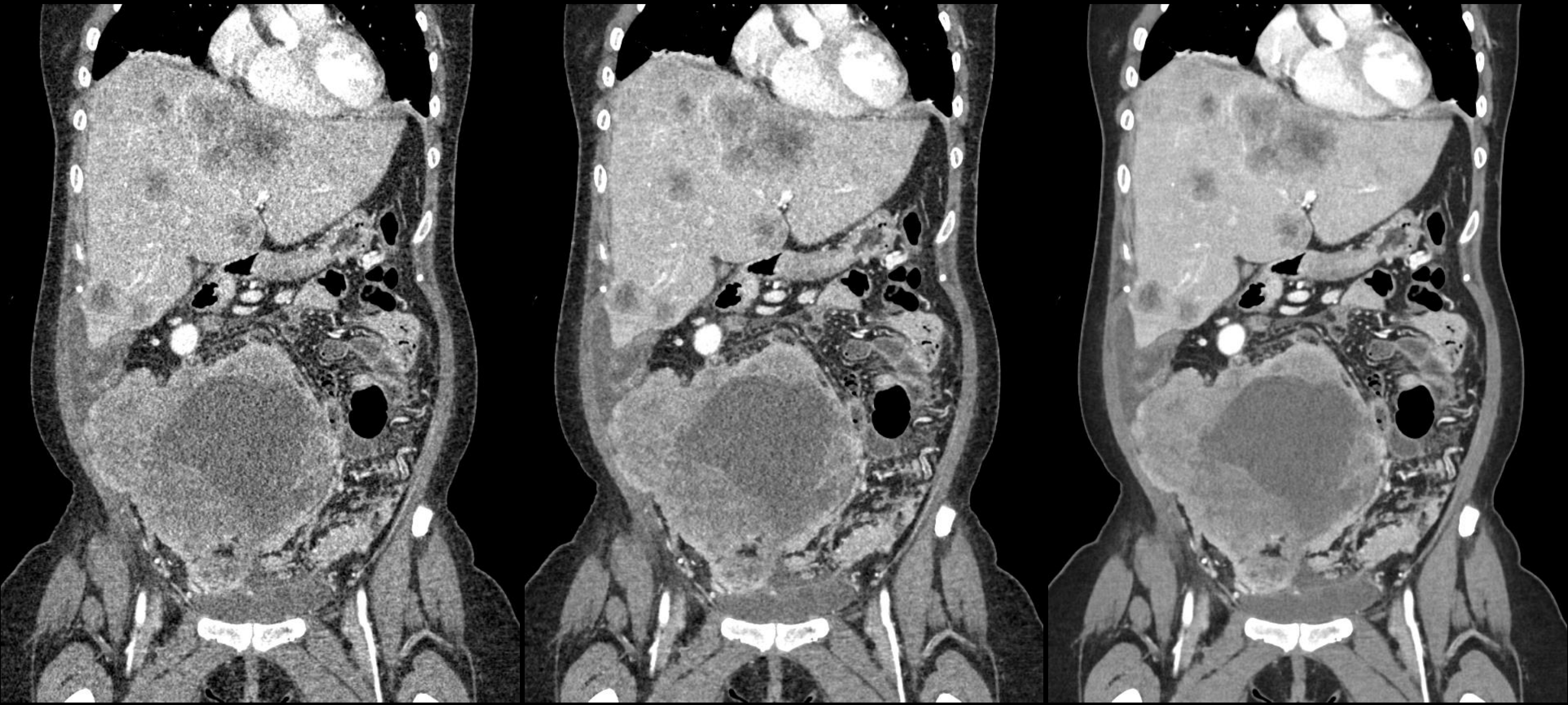

FBP ASIR V 50% True Fidelity

Courtesy of GE Healthcare

Deep Scatter Estimation

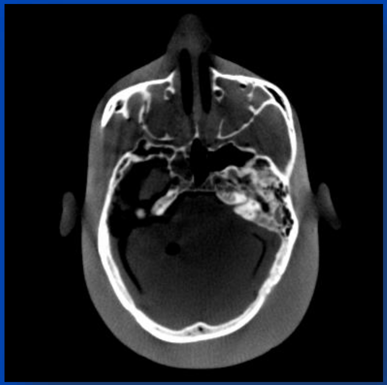

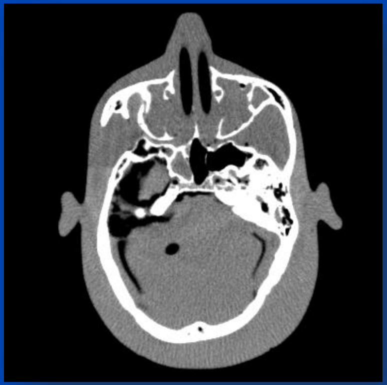

Monte Carlo Scatter Estimation

- Simulation of photon trajectories according to physical interaction probabilities.
- Simulating a large numb… ories well approximat…

1 to 10 hours
per tomographic data set

mplete scatter distribution

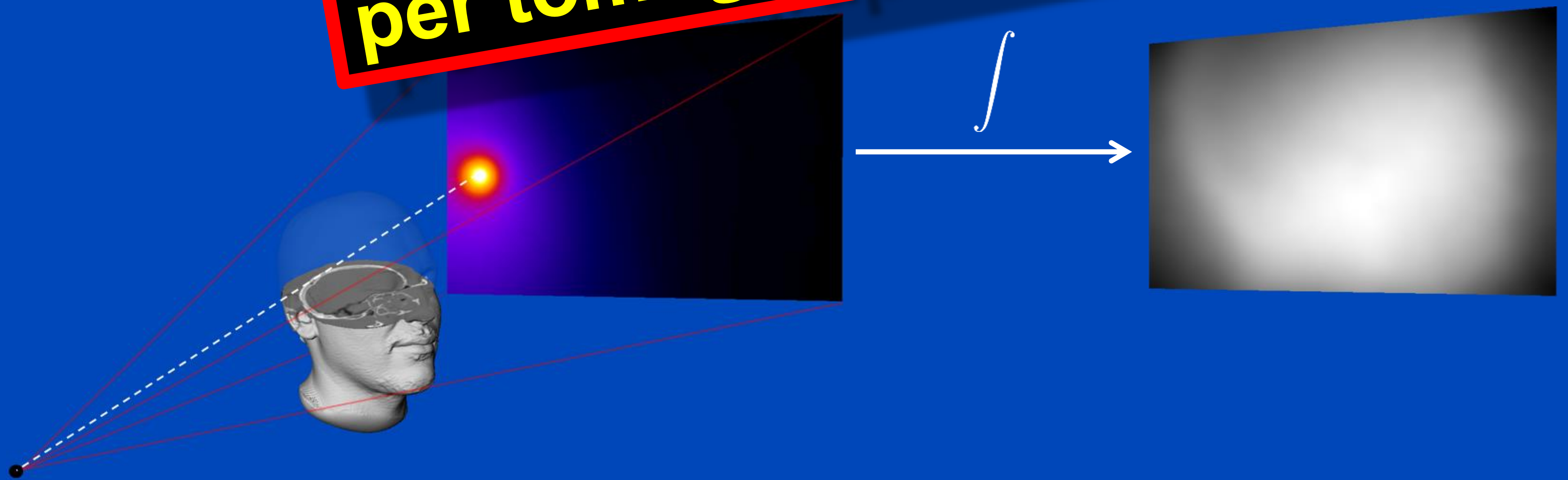

Deep Scatter Estimation (DSE)

Train a deep convolutional neural network (CNN) to estimate scatter using a functio… d projection data as in…

0.1 to 1 minute per tomographic data set

Input: $T(p)$

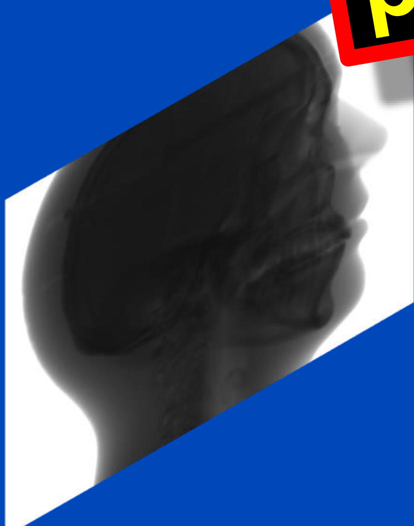

~~Monte Carlo~~

Convolutional neural network

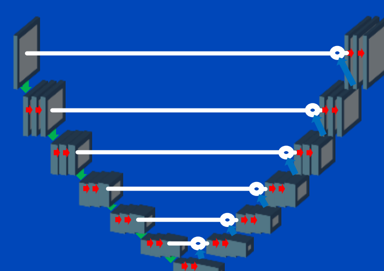

Scatter estimate

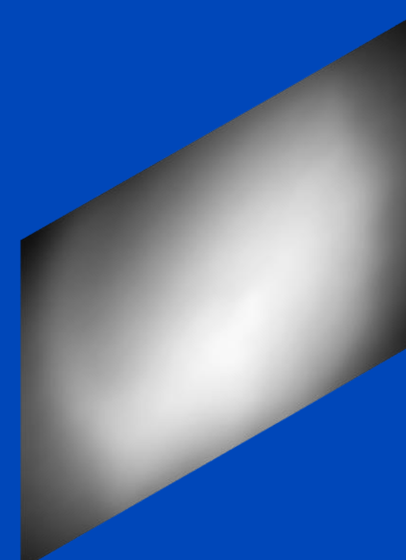

Measurement Results

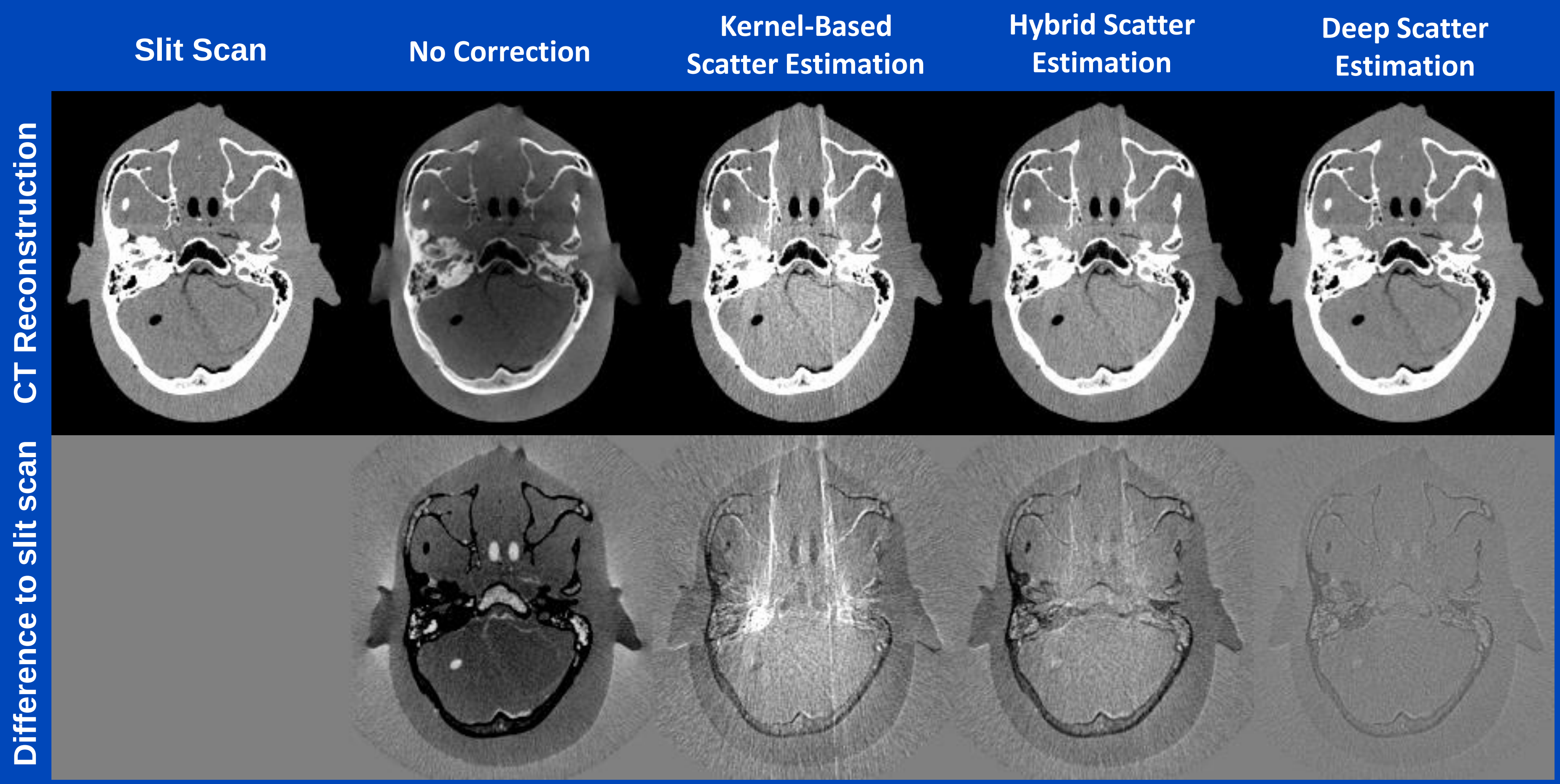

C = 0 HU, W = 1000 HU

A simple detruncation was applied to the rawdata before reconstruction. Images were clipped to the FOM before display. *C* = -200 HU, *W* = 1000 HU.

Truncated DSE[1,2]

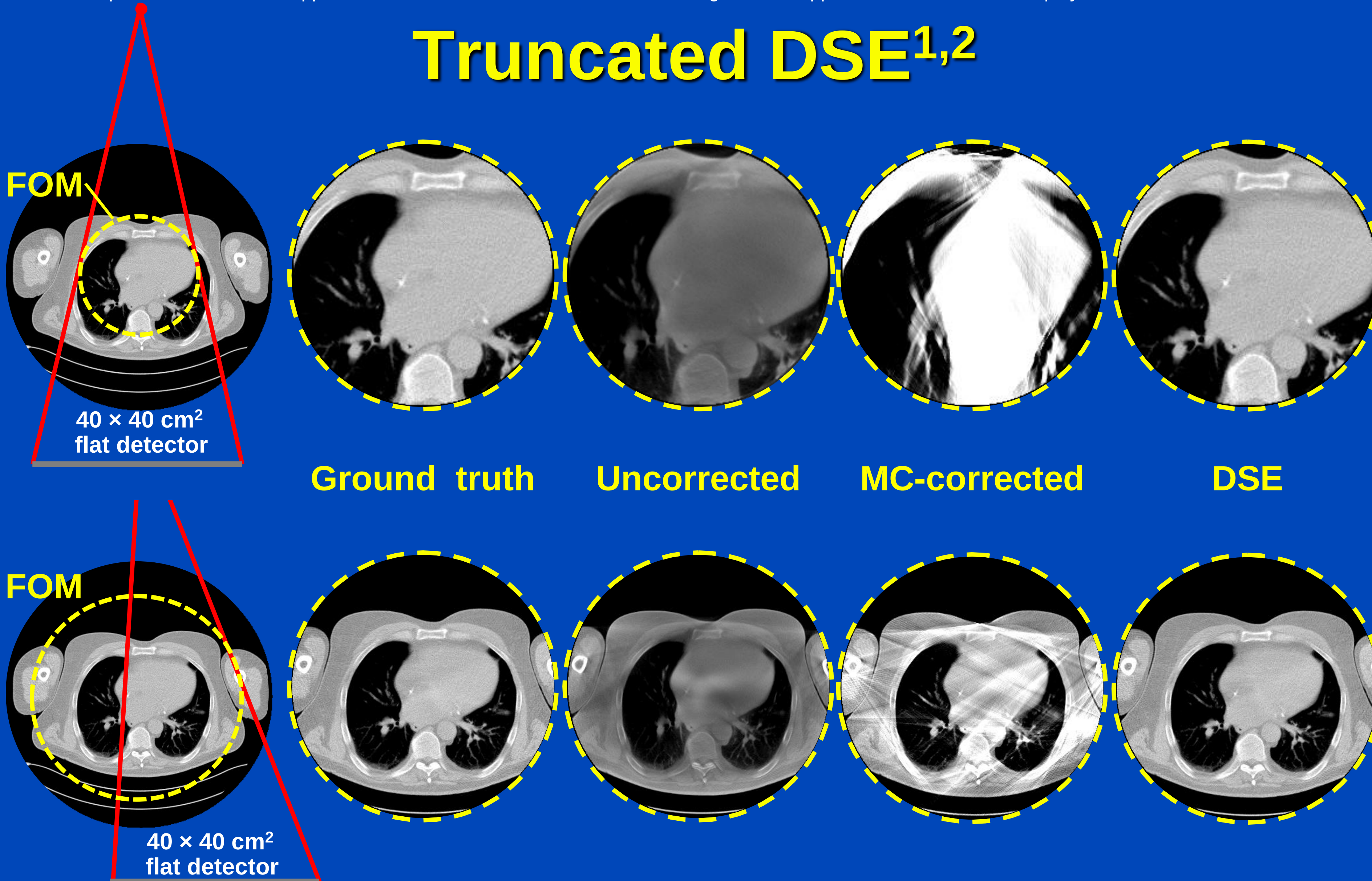

To learn why MC fails at truncated data and what significant efforts are necessary to cope with that situation see [Kachelrieß et al. Effect of detruncation on the accuracy of MC-based scatter estimation in truncated CBCT. Med. Phys. 45(8):3574-3590, August 2018].

[1]J. Maier, M. Kachelrieß et al. Deep scatter estimation (DSE) for truncated cone-beam CT (CBCT). RSNA 2018.
[2]J. Maier, M. Kachelrieß et al. Robustness of DSE. Med. Phys. 46(1):238-249, January 2019.

How Well does DSE Generalize?

DSE	Head	Thorax	Abdomen
Head	1.2	21.1	32.7
Thorax	8.8	1.5	9.1
Abdomen	11.9	10.9	1.3
All data	1.8	1.4	1.4

Values shown are the mean absolute percentage errors (MAPEs) of the testing data.
Note that thorax and head suffer from truncation due to the small size of the 40×30 cm flat detector.

TOP DOWNLOADED PAPER 2018-2019

CONGRATULATIONS TO

Marc Kachelriess

whose paper has been recognized as one of the most read in

Medical Physics

WILEY

Real-time scatter estimation for medical CT using the deep scatter estimation: Method and robustness analysis with respect to different anatomies, dose els, tube voltages, and data truncation

Joscha Maier,[a] Elias Eulig, and Tim Vöth
German Cancer Research Center (DKFZ), Im Neuenheimer Feld 280, 69120, Heidelberg, Germany
Department of Physics and Astronomy, Ruprecht-Karls-University Heidelberg, Im Neuenheimer Feld 226, 69120, Heidelberg, Germany

Michael Knaup and Jan Kuntz
German Cancer Research Center (DKFZ), Im Neuenheimer Feld 280, 69120, Heidelberg, Germany

Stefan Sawall and Marc Kachelrieß
German Cancer Research Center (DKFZ), Im Neuenheimer Feld 280, 69120, Heidelberg, Germany
Medical Faculty, Ruprecht-Karls-University Heidelberg, Im Neuenheimer Feld 672, 69120, Heidelberg, Germany

(Received 25 June 2018; revised 1 October 2018; accepted for publication 29 October 2018; published 26 November 2018)

Purpose: X-ray scattering leads to CT images with a reduced contrast, inaccurate CT values as well as streak and cupping artifacts. Therefore, scatter correction is crucial to maintain the diagnostic

Deep Dose Estimation

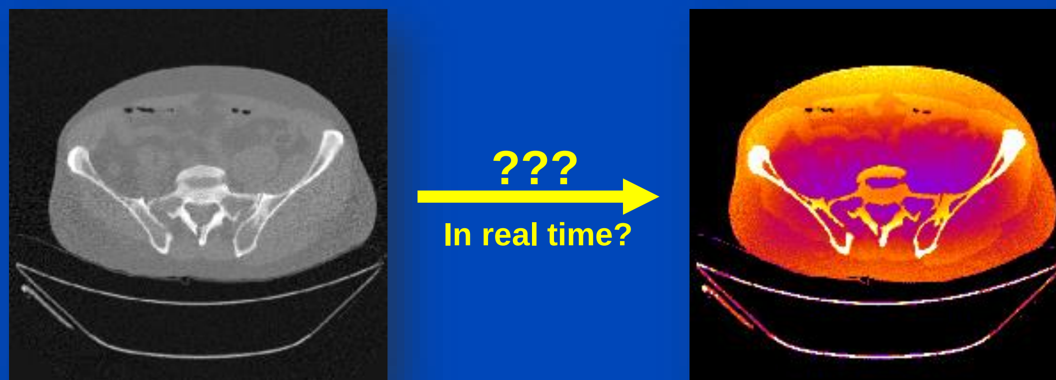

Deep Dose Estimation (DDE)

- **Combine fast and accurate CT dose estimation using a deep convolutional neural network.**
- **Train the network to reproduce MC dose estimates given the CT image and a first-order dose estimate.**

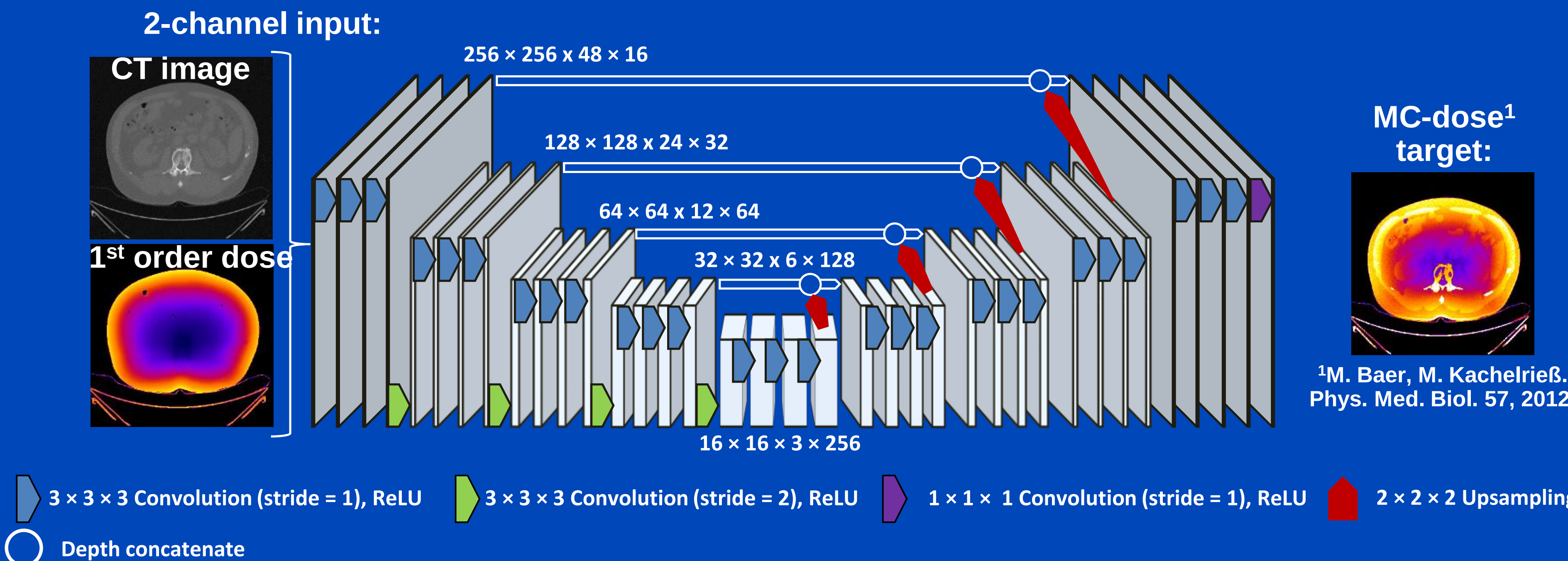

J. Maier, E. Eulig, S. Sawall, and M. Kachelrieß. Real-time patient-specific CT dose estimation using a deep convolutional neural network, Proc. IEEE MIC 2018 and ECR Book of Abstracts 2019. *Best Paper within Machine Learning at ECR 2019!*

Results

Thorax, tube A, 120 kV, no bowtie

CT image

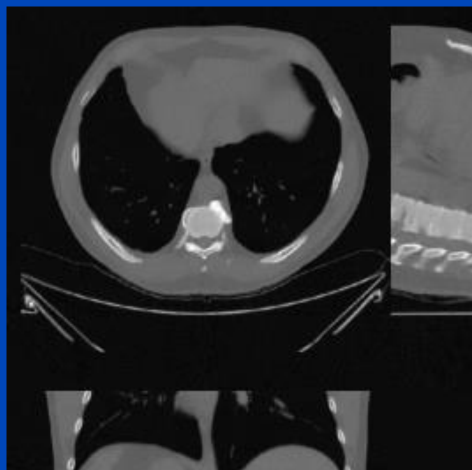

First order dose

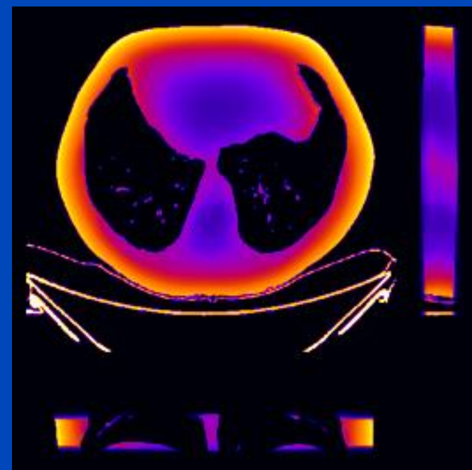

	MC	DDE
48 slices	1 h	0.25 s
whole body	20 h	5 s

MC uses 16 CPU kernels
DDE uses one Nvidia Quadro P600 GPU

DDE training took 74 h for 300 epochs, 1440 samples, 48 slices per sample

MC ground truth

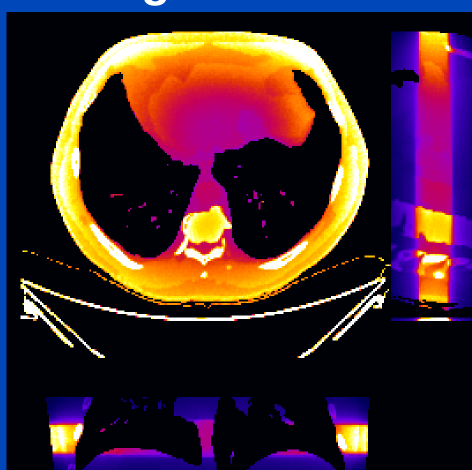

DDE

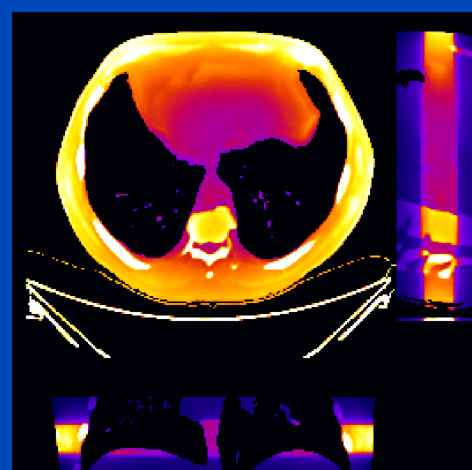

Relative error

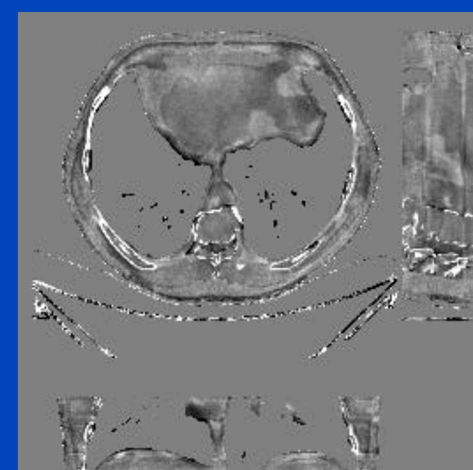

C = 0%
W = 40%

J. Maier, E. Eulig, S. Sawall, and M. Kachelrieß. Real-time patient-specific CT dose estimation using a deep convolutional neural network, Proc. IEEE MIC 2018 and ECR Book of Abstracts 2019. *Best Paper within Machine Learning at ECR 2019!*

Intervention goes Deep!

Deep DSA

???

Without mask?

Methods

General principle

Conventional DSA

I_t $-$ I_0 $=$ $\tilde{I}_t$

Deep DSA

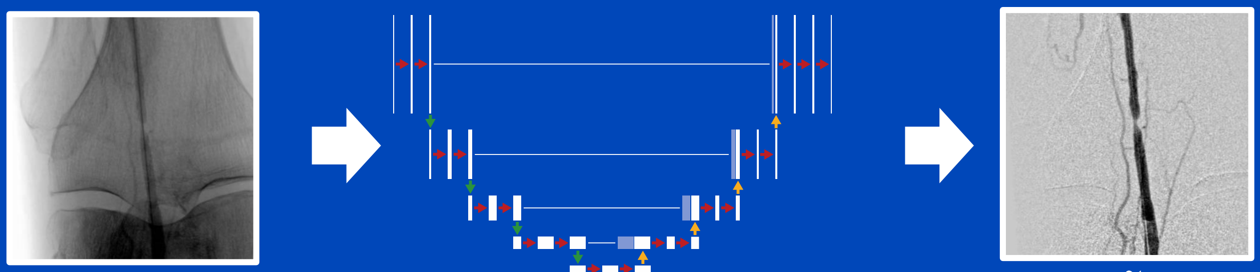

I_t $\tilde{I}_t$

- **Train on static cases where ground truth is conventional DSA**

E. Eulig, M. Kachelrieß, et al. "Learned digital subtraction angiography (Deep DSA): method and application to lower extremities". Proc. SPIE 11072, 15th International Meeting on Fully Three-Dimensional Image Reconstruction, 1107223:1-4, May 2019.

Methods
General principle

Conventional DSA

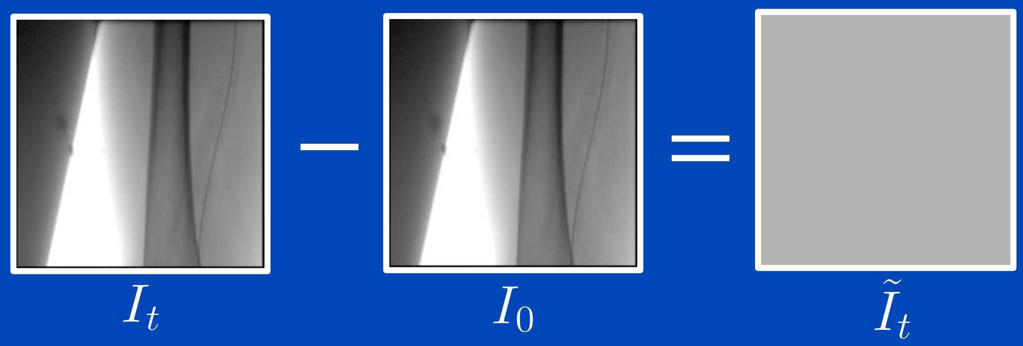

Deep DSA

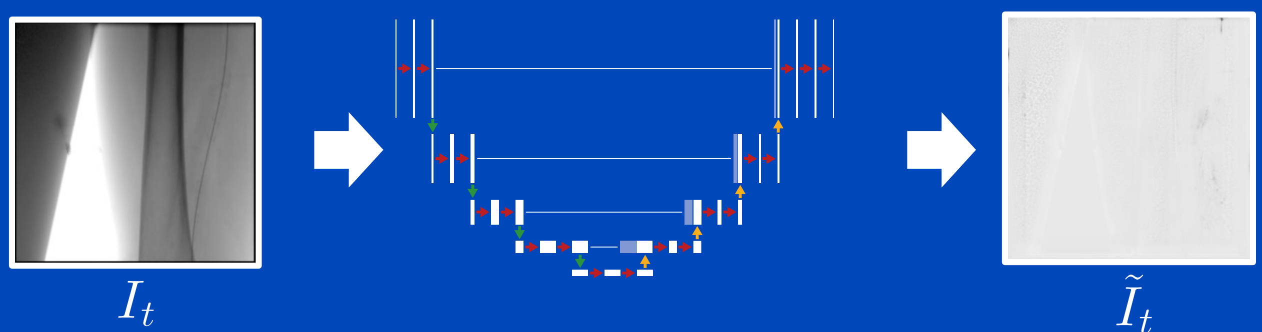

- **Train on static cases where ground truth is conventional DSA**
- **During inference CNN can be applied to both static and dynamic cases**

E. Eulig, M. Kachelrieß, et al. "Learned digital subtraction angiography (Deep DSA): method and application to lower extremities". Proc. SPIE 11072, 15th International Meeting on Fully Three-Dimensional Image Reconstruction, 1107223:1-4, May 2019.

Results

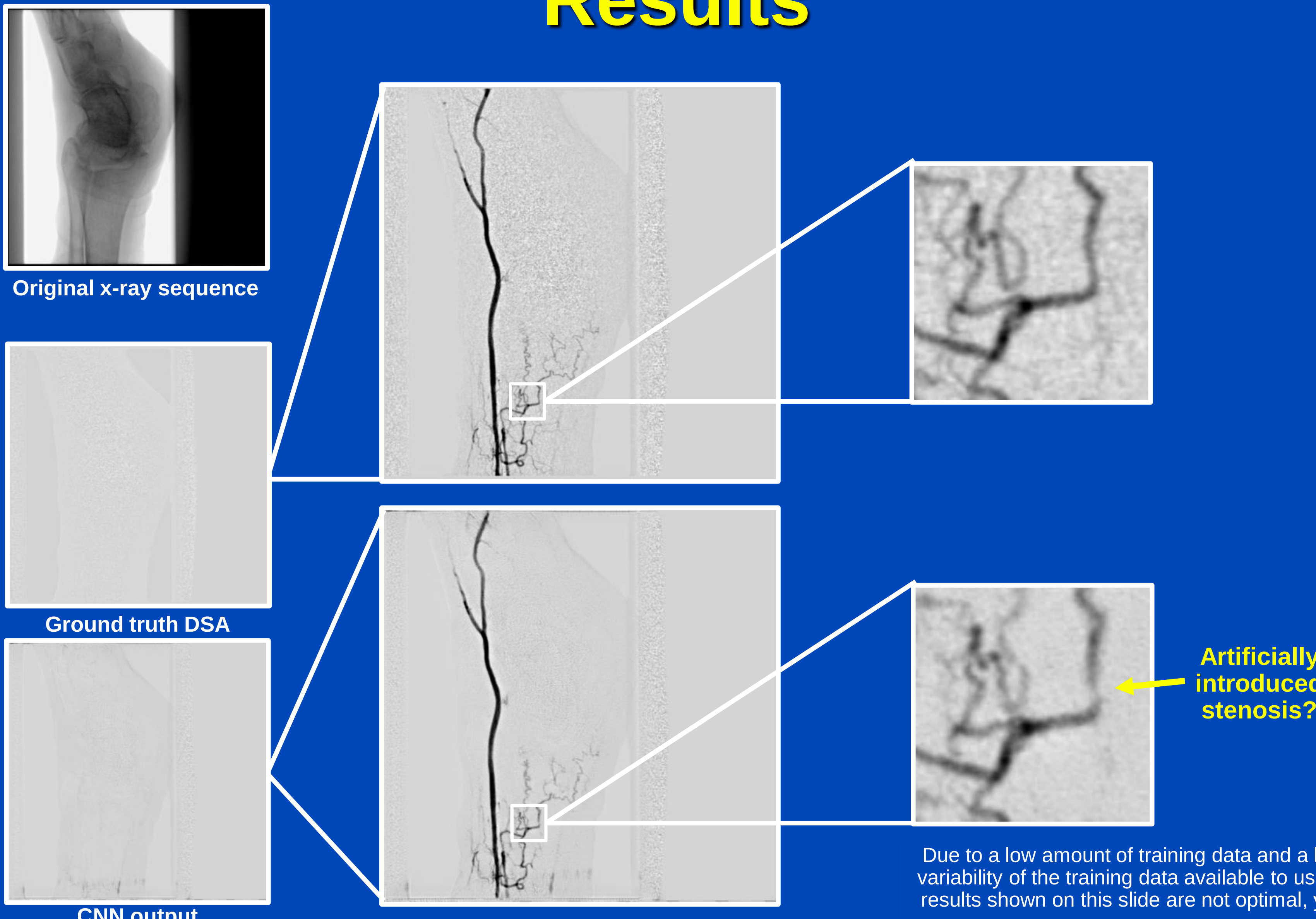

Due to a low amount of training data and a low variability of the training data available to us the results shown on this slide are not optimal, yet.

E. Eulig, M. Kachelrieß, et al. "Learned digital subtraction angiography (Deep DSA): method and application to lower extremities". Proc. SPIE 11072, 15th International Meeting on Fully Three-Dimensional Image Reconstruction, 1107223:1-4, May 2019.

Deep DSA

Fluoroscopy	DSA (fluoro minus mask)	Deep DSA (from fluoro only)

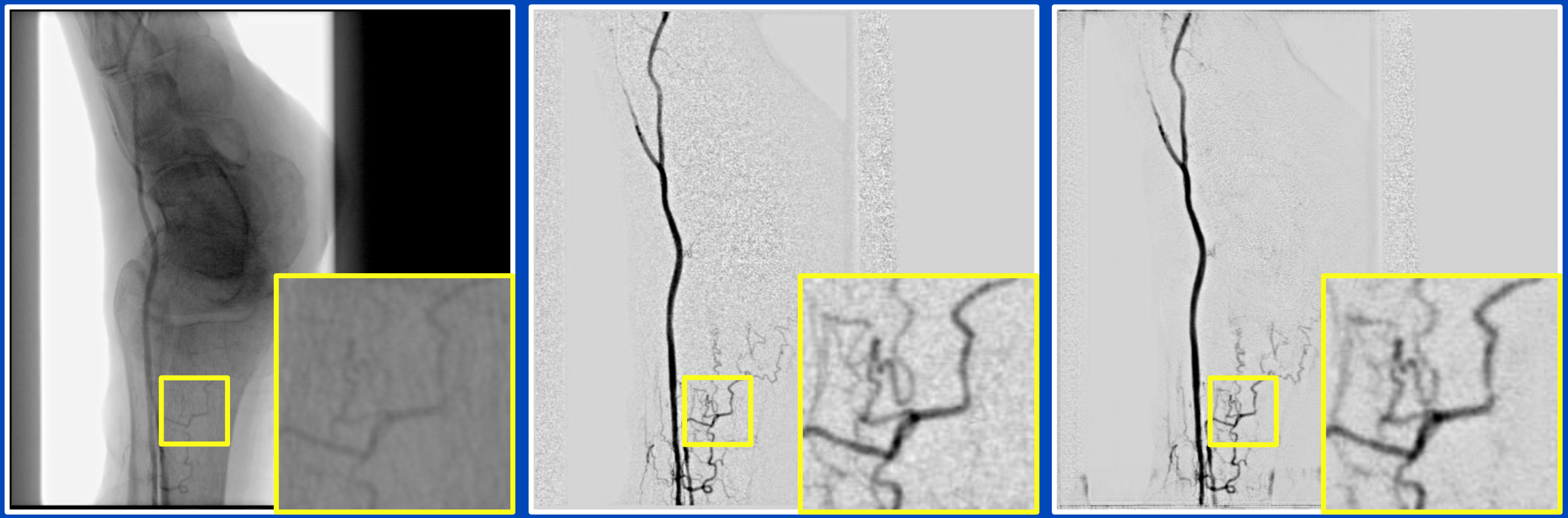

Due to a low amount of training data and a low variability of the training data available to us the results shown on this slide are not optimal, yet.

E. Eulig, M. Kachelrieß, et al. "Learned digital subtraction angiography (Deep DSA): method and application to lower extremities". Proc. SPIE 11072, 15th International Meeting on Fully Three-Dimensional Image Reconstruction, 1107223:1-4, May 2019.

Results

Bolus chase study

Dynamic fluoroscopy

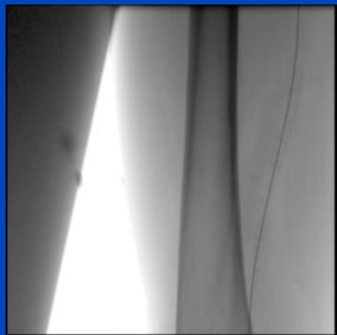

Conventional DSA

Conventional DSA infeasible due to C-arm motion

Deep DSA

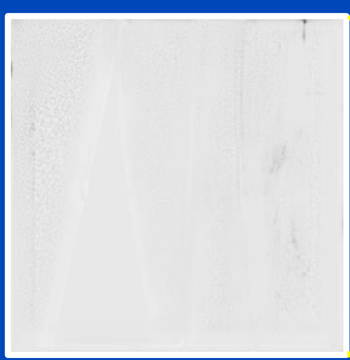

Deep DSA at t $= t_a$

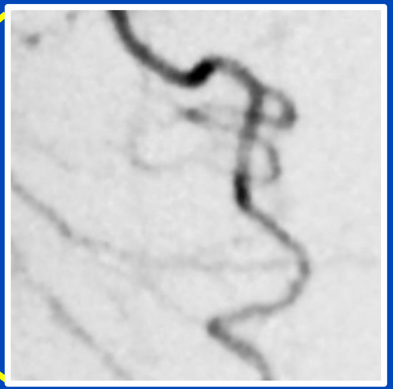

Deep DSA at t $= t_a$

E. Eulig, M. Kachelrieß, et al. "Learned digital subtraction angiography (Deep DSA): method and application to lower extremities". Proc. SPIE 11072, 15th International Meeting on Fully Three-Dimensional Image Reconstruction, 1107223:1-4, May 2019.

Deep 3D+T Tomographic Fluoroscopy

either 2D+T fluoroscopy

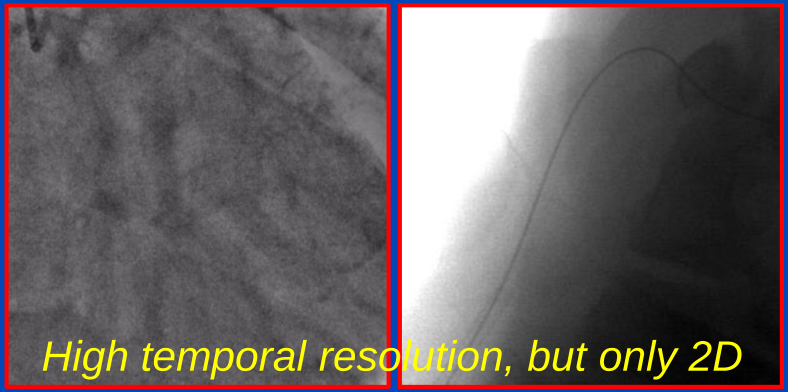

or 3D tomography

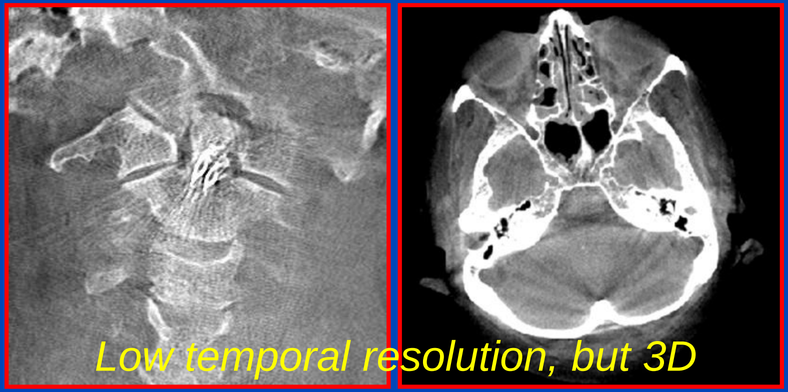

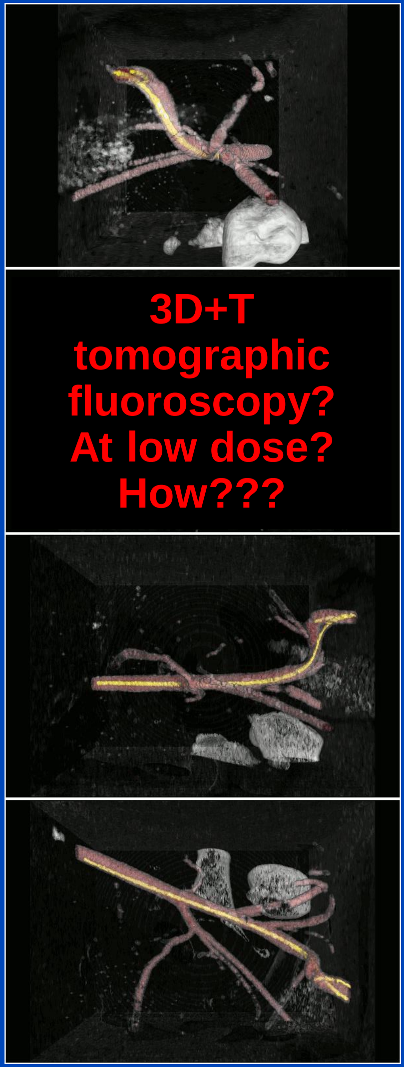

How to Realize 3D+T Fluoroscopy

- **Low dose by:**
  - Low tube current
  - Very few projections (pulsed mode)
- **Advantages of intervention guidance:**
  - Repetitive scanning of the same body region: changes are sparse.
  - Interventional materials are fine structures (few voxels) of high contrast (metal).

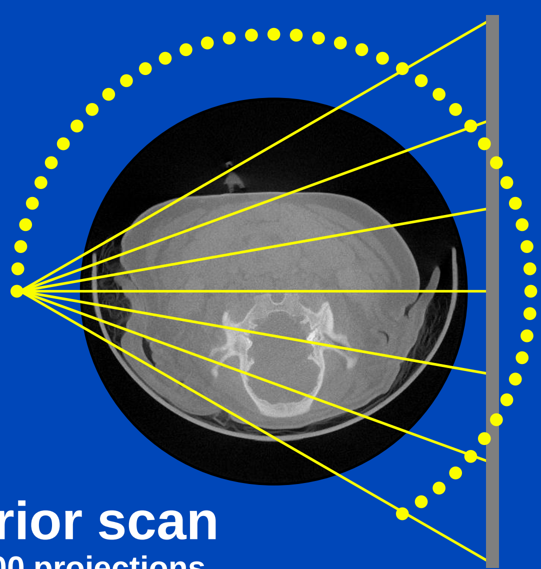

Prior scan
400 projections

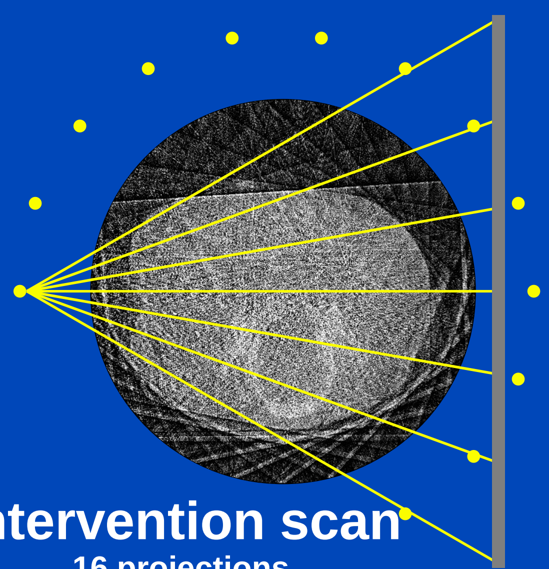

Intervention scan
16 projections

Experimental setup

J. Kuntz, M. Kachelrieß et al., "Real-time x-ray-based 4D image guidance", EuRad 23:1669–1677, January 2013.
J. Kuntz, M. Kachelrieß et al., "Constrained reconstructions for 4D intervention guidance". PMB 58:3283–3300, April 2013.
B. Flach, M. Kachelrieß et al., "Low dose tomographic fluoroscopy", MedPhys 40:101909, 11 pages, October 2013.

2013: 3D+T Fluoroscopy at Low Dose

Guide Wire in the Carotis of a Pig with Angio Roadmap Overlay

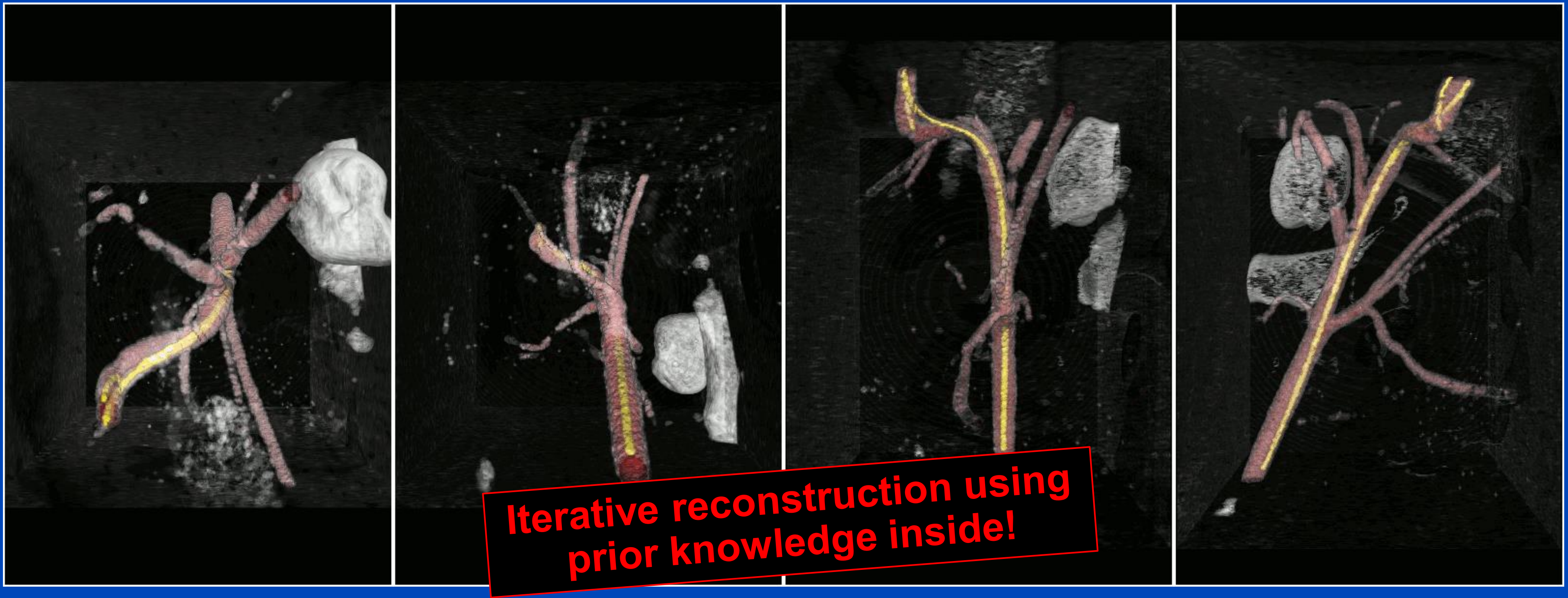

This work was awarded the intervention award 2013 of the German Society of Neuroradiology (DGNR).
This work was further selected as the Editor's Pick for the Medical Physics Scitation site.

- Dose of the 2013 approach: 20 bis 50 µGy/s.
- This is about 4 to 8 times higher than 2D fluoroscopy.
- Need to reduce number of projections from 16 to 4.
- How? → Deep Learning!

J. Kuntz, M. Kachelrieß et al., "Real-time x-ray-based 4D image guidance", EuRad 23:1669–1677, January 2013.
J. Kuntz, M. Kachelrieß et al., "Constrained reconstructions for 4D intervention guidance". PMB 58:3283–3300, April 2013.
B. Flach, M. Kachelrieß et al., "Low dose tomographic fluoroscopy", MedPhys 40:101909, 11 pages, October 2013.

Method

Deep Tool Extraction (DTE), Feldkamp Recon (FDK), Deep Tool Reconstruction (DTR)

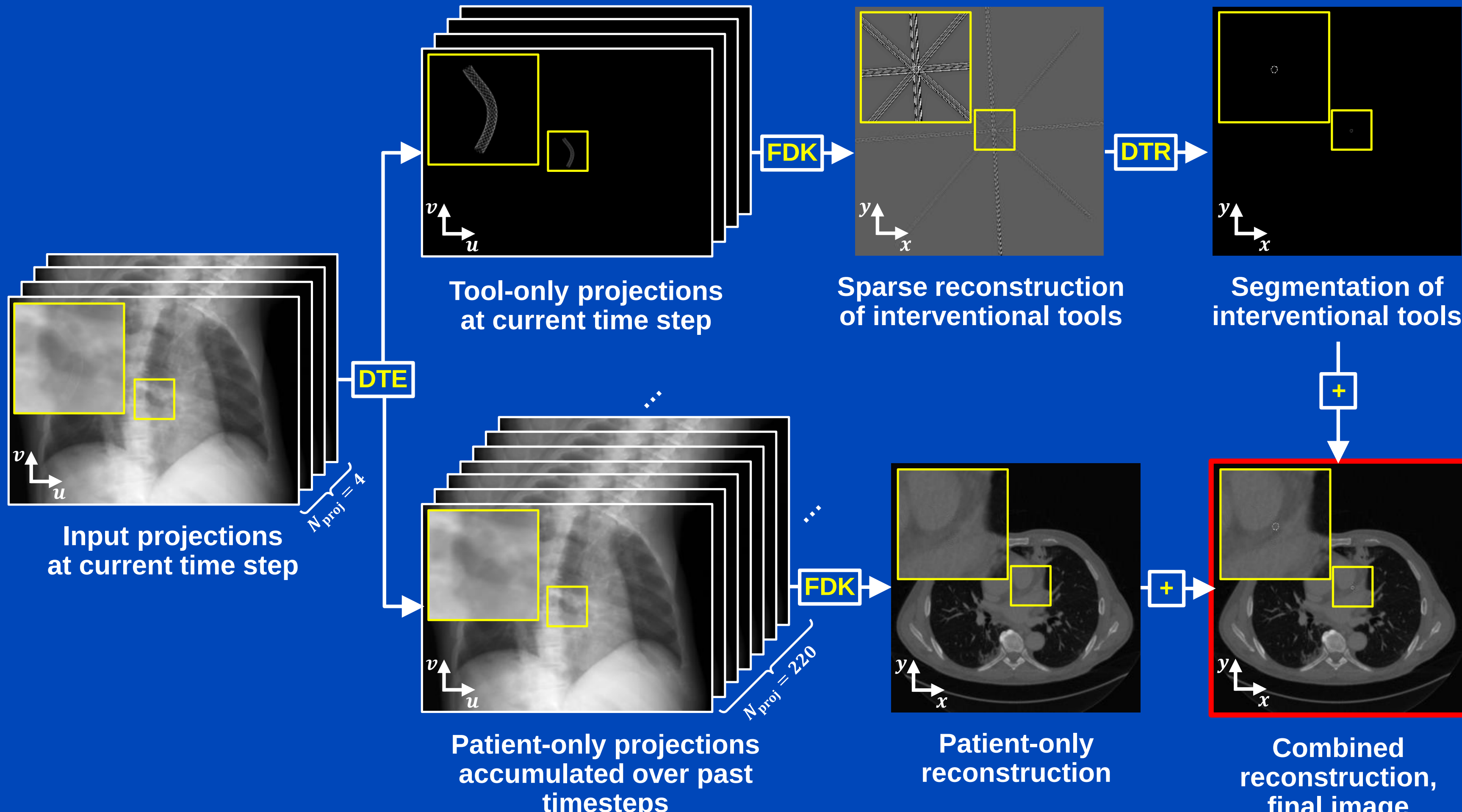

E. Eulig, J. Maier, N.R. Bennet, M. Knaup, K. Hörndler, A. Wang, and M. Ka-chelrieß. Deep learning-aided CBCT image reconstruction of interventional material from four x-ray projections. SPIE Medical Imaging Conference Record, 113121L:1-7, March 2020.

Zeego Measurements with Just 4 Projections

Ground truth (measurements from 400 projections)

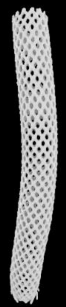

Details siehe Preisübergabe des Dietrich-Harder Masterarbeitspreises an

Elias Eulig

Freitag 11:40, Behnken-Berger-Sitzung

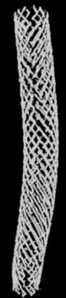

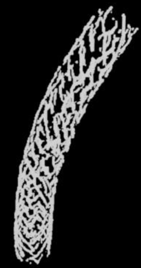

Loop through slices reconstructed from just 4 projections without AI:

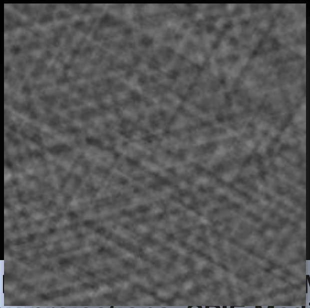

Stent examples:

E. Eulig, J. Maier, N.R. Bennet, M. Knaup, K. M. Ka-chelrieß. Deep of interventional material from four x-ray projections. SPIE Medical Imaging Conference Record, 113121L:1-7, March 2020.

Motion Compensation

3D CBCT	**4D gated CBCT**	**sMoCo**	**acMoCo**
Standard	Conventional Phase-Correlated	Standard Motion Compensation	**Artifact Model-Based Motion Compensation**

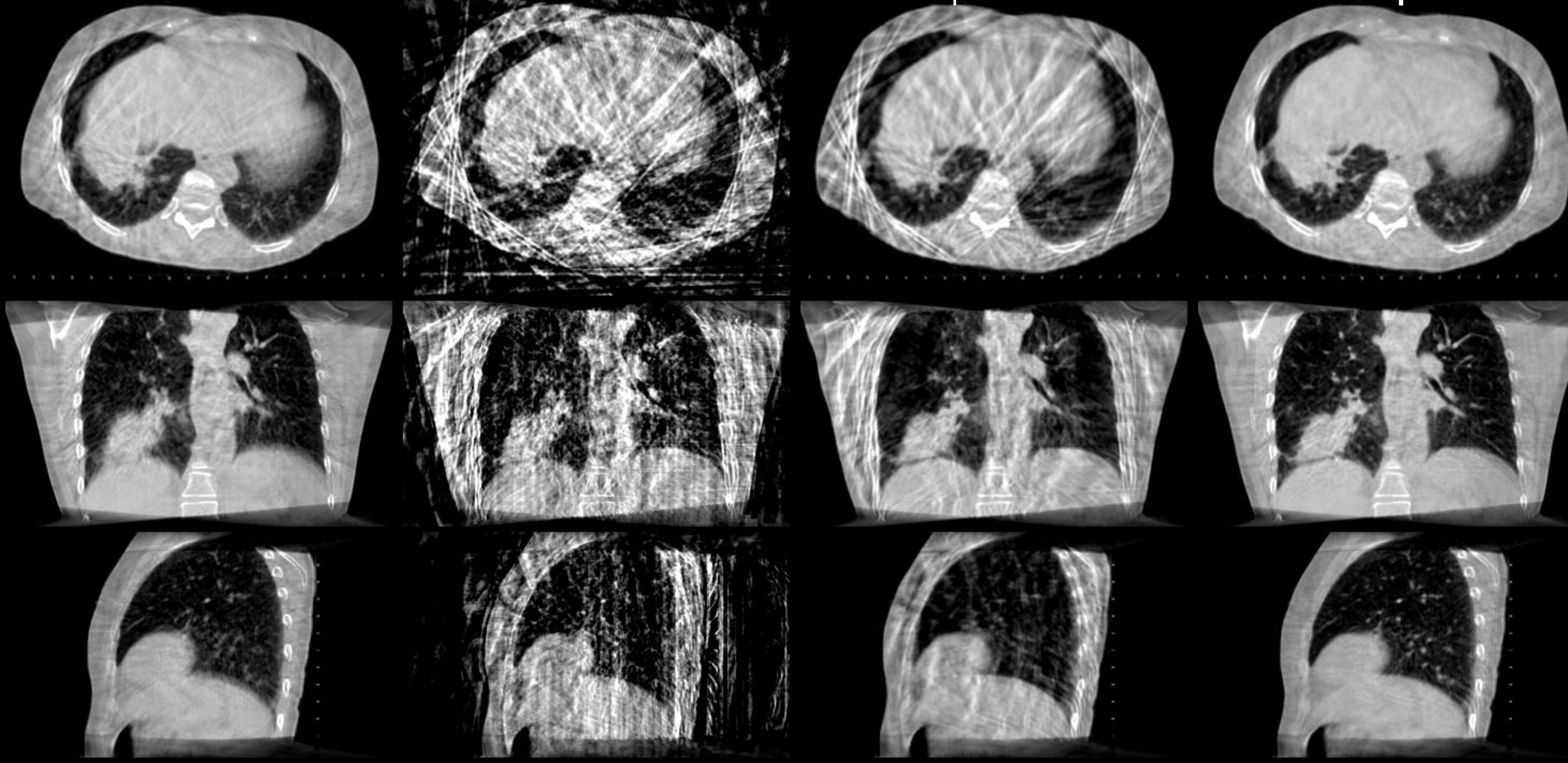

***C* = -200 HU, *W* = 1400 HU, displayed with 30 rpm.**
Patient data provided by Memorial Sloan–Kettering Cancer Center, New York, NY.

Brehm, Kachelrieß et al., “Self-adapting cyclic registration for CBCT”, Med. Phys. 39(12):7603-7618, 2012.
Brehm, Kachelrieß et al., “Artifact-resistant motion estimation for CBCT” Med. Phys. 40(10):101913, 2013.
Brehm, Kachelrieß et al., “Cardio-respiratory motion-compensated micro-CT” Med. Phys. 42(4):1948-1958, 2015.

Deep Cardiac Motion Compensation

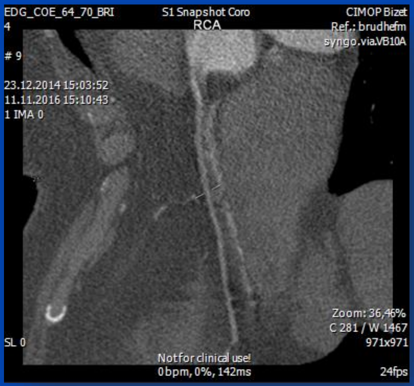

???

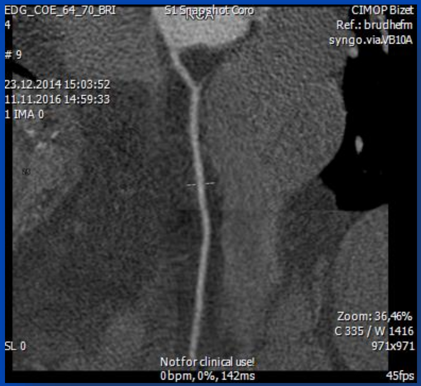

Motion Compensation for Cardiac CT

Input: CT image with motion artifacts

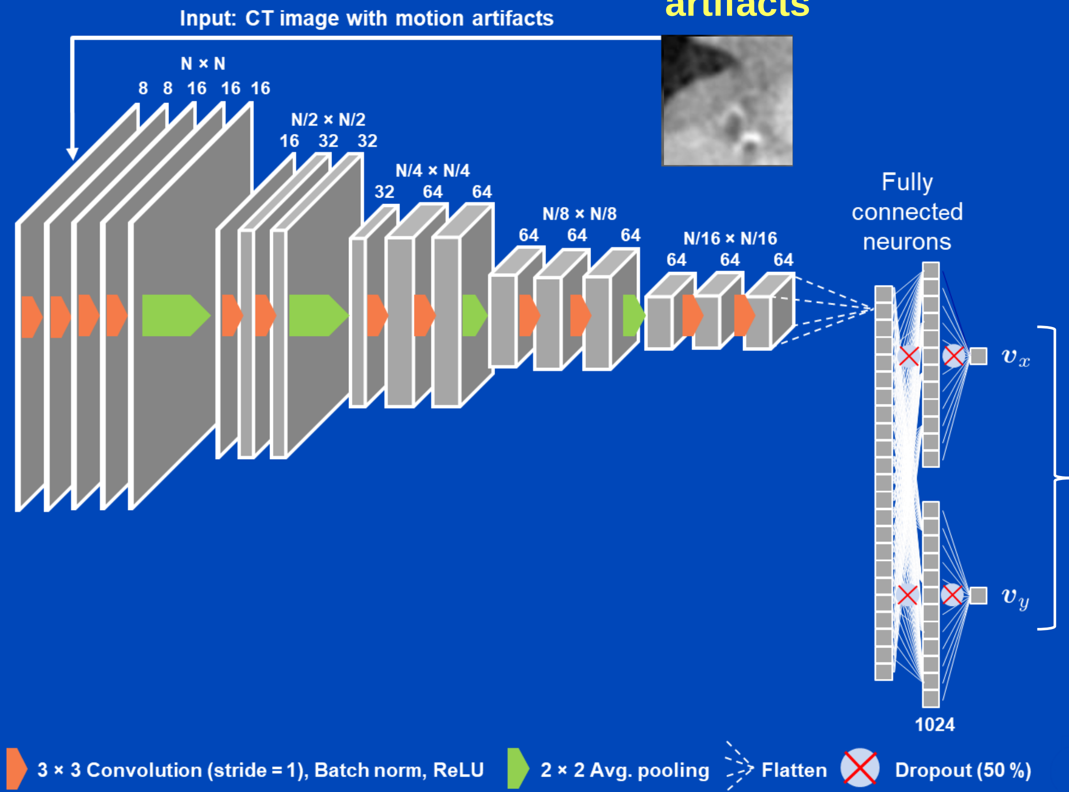

Output: motion direction (to be used by MoCo recon)

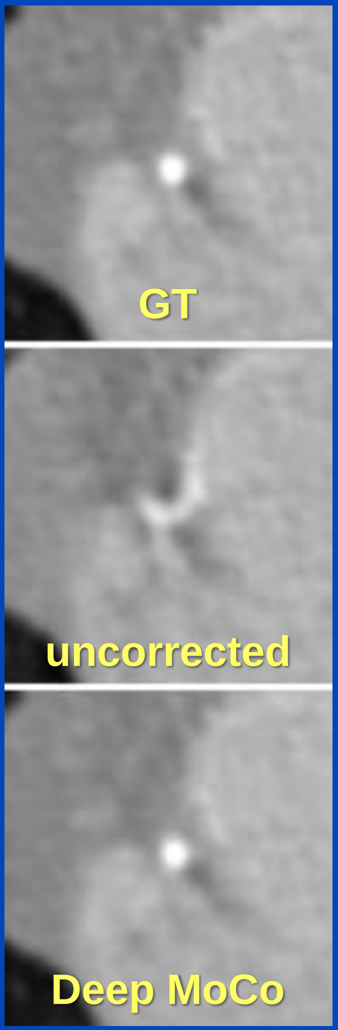

J. Maier, S. Lebedev, E. Eulig, S. Sawall, E. Fournié, K. Stierstorfer, and M. Kachelrieß. Coronary artery motion compensation for short-scan cardiac CT using a spatial transformer network. Conference Program of the 6th International CT-Meeting, August 2020.

Results

Measurements, patient 1

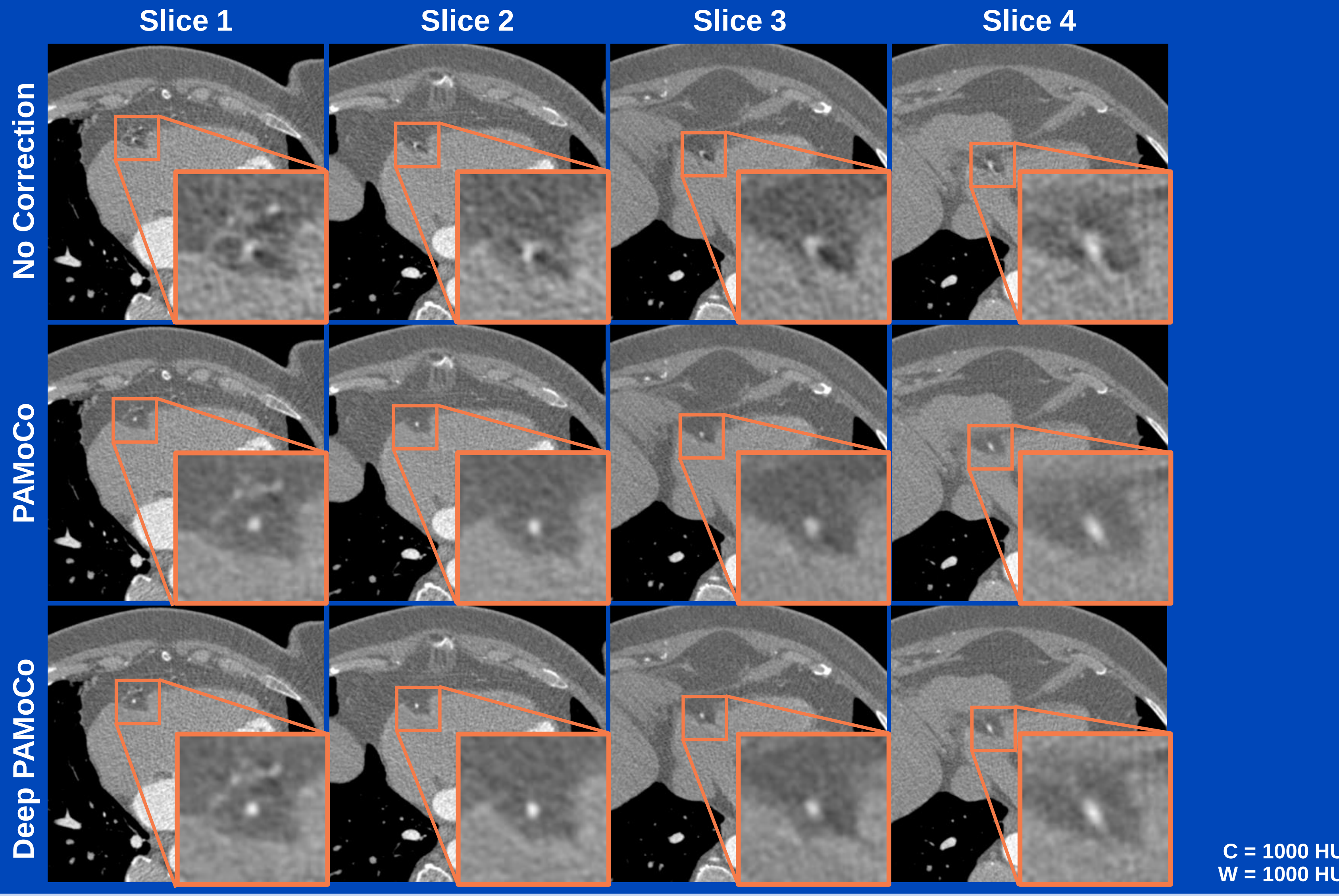

J. Maier, S. Lebedev, E. Eulig, S. Sawall, E. Fournié, K. Stierstorfer, and M. Kachelrieß. Coronary artery motion compensation for short-scan cardiac CT using a spatial transformer network. Conference Program of the 6th International CT-Meeting, August 2020.

Results

Measurements, patient 2

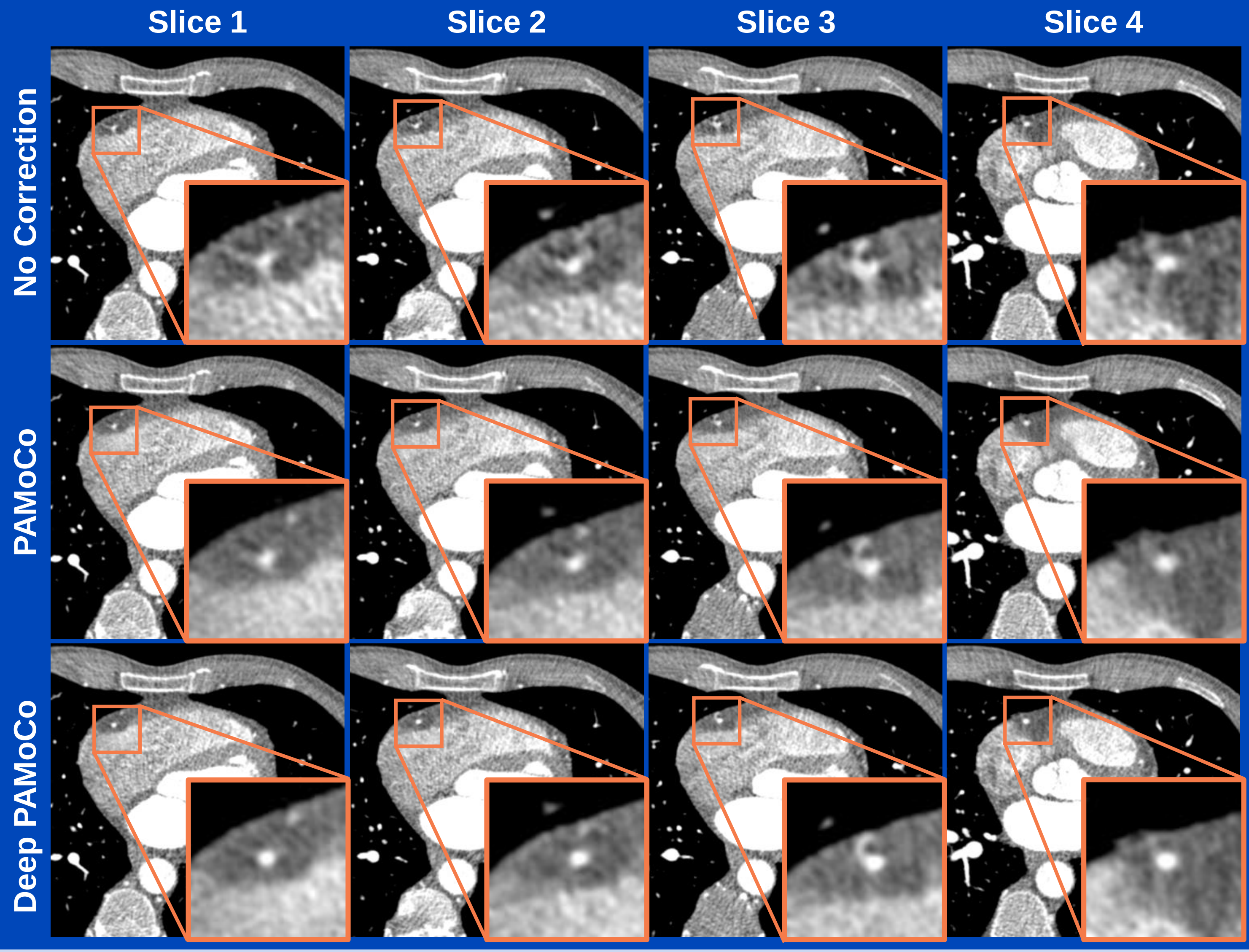

C = 1000 HU
W = 1000 HU

J. Maier, S. Lebedev, E. Eulig, S. Sawall, E. Fournié, K. Stierstorfer, and M. Kachelrieß. Coronary artery motion compensation for short-scan cardiac CT using a spatial transformer network. Conference Program of the 6th International CT-Meeting, August 2020.


Vielen Dank
This presentation will soon be available at www.dkfz.de/ct.
Job opportunities through DKFZ’s international PhD or
Postdoctoral Fellowship programs
(marc.kachelriess@dkfz.de).